Reviews on Advanced Materials and Technologies, 2026, vol. 8, no. 1, pp. 30–64
DOI: 10.17586/2687-0568-2026-8-1-30-64

Architectural Design Strategies in Ceramic–Polymer Hybrid Piezoelectric Composites for Enhanced Energy Harvesting Performance

A. Jaberi *, **E.N. Dresvyanina**

Institute of Textiles and Fashion, Saint Petersburg State University of Industrial Technologies and Design, Bolshaya Morskaya, 18, Saint Petersburg, 191186, Russia

Article history

Received February 27, 2026
Received in revised form
March 15, 2026
Accepted March 16, 2026
Available online March 26, 2026

Abstract

Ceramic–polymer piezoelectric composites integrate the high piezoelectric activity of ferroelectric ceramics with the mechanical flexibility and durability of polymers, forming a key platform for next-generation energy harvesting. This review critically examines recent progress in hybrid composites for mechanical-to-electrical energy conversion, emphasizing architectural design strategies that govern structure–property–performance relationships. Particular focus is placed on connectivity patterns (0–3, 1–3, and 3–3) and advanced engineering approaches—including aligned ceramic networks, porous scaffolds, core–shell structures, gradient configurations, and interfacial functionalization—which enhance stress transfer, electromechanical coupling, and power density while reducing brittleness and dielectric loss. Lead-based (e.g., PZT) and lead-free systems (e.g., BTO, KNN), combined with flexible matrices such as PVDF and its copolymers, are assessed for applications in low-frequency vibrations, wearable electronics, structural health monitoring, and self-powered sensors. Scalable fabrication methods (freeze casting, electrospinning, 3D printing) and multiphysics modelling are evaluated alongside major challenges: polarization stability, fatigue resistance, interfacial debonding, and long-term reliability. The review provides a unified framework for architectural optimization and strategic directions toward efficient, robust, and sustainable energy harvesters.

Keywords: Ceramic–polymer piezoelectric composites; Energy harvesting; Composite architecture; Connectivity (0–3, 1–3, 3–3); Structural health monitoring

1. INTRODUCTION

The piezoelectric effect—the linear electromechanical coupling in non-centrosymmetric crystalline systems manifested through charge generation under mechanical stress and conversely mechanical strain under an applied electric field—is foundational to a broad range of sensing, actuation, and energy conversion technologies. Since its initial characterization in quartz by the Curie brothers and subsequent application in barium titanate ($BaTiO_3$) and lead zirconate titanate (PZT) in the mid-20th century, piezoelectric transducers have been integral to precision instrumentation [1]. In recent decades (Table 1), interest has pivoted toward piezoelectric energy harvesting as a sustainable strategy for powering distributed electronics and wireless sensor networks by capturing low-frequency ambient vibrations from structural, fluidic, and biomechanical sources. These vibrations are pervasive but low in magnitude (typically < 100 Hz), requiring materials with high electromechanical coupling efficiency and mechanical adaptability [2].

Energy harvesting technologies exploit various ambient energy sources, including solar radiation, thermal gradients, electromagnetic fields, and mechanical vibrations, each characterized by distinct power density ranges depending on environmental conditions and device configuration (Table 2). Photovoltaic systems generally provide the highest power densities, reaching tens to hundreds of mW/cm^2 under direct sunlight and several mW/cm^2 under indoor illumination. Thermoelectric generators typically operate within the range of approximately 10–1000 $\mu W/cm^2$ depending on the available temperature gradient, whereas electromagnetic and electrostatic vibration harvesters commonly generate power densities on the order of 1–1000 $\mu W/cm^3$ under resonant mechanical excitation. Piezoelectric energy harvesting systems, in contrast, generally produce power densities ranging from several to tens of $\mu W/cm^3$ depending on excitation frequency, strain amplitude, and

* Corresponding author: A. Jaberi, e-mail: dzhaberi.a.679@suitd.ru

Table 1. Representative developments in ceramic–polymer piezoelectric composites for energy harvesting. Following abbreviations are used: PZT – lead zirconate titanate, PZT5A4 – soft lead zirconate titanate, PDMS – polydimethylsiloxane, PZN – lead zinc niobate, KNN – potassium sodium niobate, $Ba_{0.5}Sr_{0.5}TiO_3$ – barium strontium titanate, BNT – bismuth sodium titanate, PVDF–TrFE – poly(vinylidene fluoride-trifluoroethylene), CNTs – carbon nanotubes. Based on Refs. [2–7].

Year	Architecture / Connectivity	Ceramic phase	Polymer matrix	Fabrication method	Key performance metrics	Notable contribution
1978	0–3 particulate composite	PZT	PVDF	Conventional mixing & hot pressing	$d_{33} \approx 40$–70 pC/N	First systematic connectivity model (Newnham connectivity theory)
1990s	1–3 fiber composite	PZT	Epoxy	Dice-and-fill	$k_t > 0.4$; d_{33} up to 300 pC/N	Reduced clamping, improved electromechanical coupling
2001	3–3 interconnected composite	PZT	Polymer infiltration	Injection/infiltration	Enhanced stress transfer vs 0–3	Continuous ceramic pathways for improved coupling
2011	Di-electrophoresis aligned structured composite (DEP)	PZT5A4	Polyurethane	Dielectrophoretic alignment	~ 10× energy density improvement	Field-assisted alignment enhances stress transfer
2018	3D foam-templated (3–3)	PZT (~ 16 vol.%)	PDMS	PU template infiltration + sintering	85 V under 8% compressive strain	Cellular skeleton architecture improves voltage output
	Biomimetic porifera-inspired (3–3)	PZT-based	Elastomer	Freeze casting / templating	~ 16× power output increase	Nature-inspired load distribution enhances efficiency
2020	Ice-templated 2–2 skeleton	PZN-PZT	PDMS	Freeze casting	$d_{33} \cdot g_{33} = 58.213 \times 10^{-15}$ m^2/N	Exceptional transduction coefficient via aligned lamellae
2022	3D interpenetrating phase composite (IP3C)	PZT	PDMS	Camphene-templated freeze casting	7× d_{33} improvement	Independent stress transfer from stiffness ratio
2023	Vertically aligned microchannels	PZT + CNTs	PVDF	Phase inversion	$d_{33} = 595$ pC/N; 66 V; 1.25 μW/mm^2	Synergistic CNT-enhanced polarization
	Layered hybrid thin-film composite	$Ba_{0.5}Sr_{0.5}TiO_3$	PVDF-TrFE	RF sputtering + spray deposition	> 3× power increase	Interfacial nanolayer engineering
2024	Lead-free hierarchical composite	KNN / BNT-based	Elastomer	3D printing / freeze casting	Comparable to PZT-based at moderate loading	Toward environmentally sustainable systems

Table 2. Typical power density ranges of major ambient energy harvesting sources.

Energy source	Typical power density	Key characteristics	Representative applications
Solar (photovoltaic)	10–100 mW/cm^2 (sunlight)	Highest energy density but dependent on illumination	Outdoor sensors, portable electronics
Thermoelectric	10–1000 μW/cm^2	Requires temperature gradient	Industrial monitoring, waste heat recovery
Electromagnetic vibration	10–1000 μW/cm^3	Effective at higher frequencies	Machinery monitoring
Electrostatic	1–100 μW/cm^3	MEMS-compatible systems	Microelectronics
Piezoelectric vibration	1–100 μW/cm^3	High efficiency under mechanical excitation	Wearables, SHM sensors, biomedical devices

material configuration. Although their absolute power output may be lower than that of photovoltaic systems, piezoelectric harvesters offer a decisive advantage in environments where mechanical vibrations, cyclic stresses, or biomechanical motions are continuously available. These conditions are particularly relevant for distributed sensor networks, wearable electronics, structural health monitoring systems, and implantable biomedical devices. Consequently, the development of high-performance piezoelectric materials capable of efficiently converting

low-frequency mechanical energy into electrical power has become an important research focus, with ceramic–polymer hybrid composites emerging as a promising solution that combines high polarization activity with mechanical flexibility.

Ceramic piezoelectrics such as PZT, potassium sodium niobate (KNN), and modified bismuth sodium titanate (BNT) exhibit high piezoelectric coefficients (d_{33} > 200 pC/N) and strong dielectric permittivity (ε_r > 1000) conducive to high energy conversion metrics. However, their intrinsic brittleness and high elastic modulus (~ 50–100 GPa) impede integration in flexible or mechanically dynamic systems, leading to premature fracture under cyclic loading [8]. Conversely, piezoelectric polymers—notably polyvinylidene fluoride (PVDF) and its copolymers (e.g., polyvinylidene fluoride-trifluoroethylene, PVDF-TrFE)—offer high mechanical flexibility (Young's modulus ~ 1–3 GPa), low acoustic impedance, and facile processing [9]. Although, their piezoelectric coefficients are comparatively modest (d_{33} ~ −20 to −30 pC/N) with lower dielectric constants (~10–12), constraining harvested power output [10]. These complementary material attributes underpin the emergence of ceramic–polymer piezoelectric composites, designed to synergistically integrate high polarization activity with mechanical compliance.

Early composite architectures relied heavily on particulate dispersions (0–3 connectivity), where ceramic particles are embedded within a polymer matrix achieving volume fractions up to ~ 50 vol.% but suffering limited stress transfer due to discontinuous ceramic pathways [3]. These systems generally demonstrated modest piezoelectric performance enhancement (d_{33} ~ 40–70 pC/N) relative to neat PVDF owing to poor interphase coupling [11]. Recognizing these limitations, researchers advanced structured connectivities such as 1–3, 0–3, and 3–3 systems, wherein continuous ceramic fibers, lamellae, or interconnected networks promote more efficient stress transfer and polarization alignment [12]. For instance, 1–3 composites fabricated via dice-and-fill techniques exhibited up to 2× improvement in electromechanical coupling (k_t > 0.4) compared to random composites at similar ceramic loadings, attributed to reduced mechanical clamping effects and continuous load paths [13]. Beyond connectivity, advanced structuring strategies have demonstrated significant performance gains. Freeze casting produces lamellar, aligned ceramic frameworks with controlled porosity, yielding enhanced d_{33} and g_{33} coefficients through improved stress distribution and connectivity. Template-assisted infiltration and dielectrophoretic alignment create oriented ceramic phases within polymer matrices, further optimizing mechanical integrity and phase continuity. Additive manufacturing (e.g., direct ink writing) has recently enabled multimaterial scaffolds with architected porosity and graded phase distributions, reported to improve harvested power densities by > 50% relative to conventional composites. Interfacial engineering via functional coupling agents or core–shell architectures has emerged as critical for enhancing interphase adhesion, reducing dielectric loss, and stabilizing ferroelectric domains under cyclic loading [14]. Despite these advances, key challenges remain. Long-term polarization stability under mechanical fatigue, interfacial debonding, dielectric losses inherent to multiphase systems, and the transition toward environmentally benign, lead-free ceramics (e.g., KNN, BNT modified systems) persist as barriers to commercialization. Moreover, unifying effective medium theories with multiphysics models to accurately predict performance across frequency, strain amplitude, and temperature remains an active research focus [15]. This review systematically examines the interplay of architectural design, phase connectivity, and interfacial engineering in ceramic–polymer piezoelectric composites, elucidating structure–property–performance relationships critical to advancing high-efficiency mechanical energy harvesters stable under real-world conditions.

2. MATERIAL SELECTION AND HYBRID COMPOSITE DESIGN

The performance of ceramic–polymer hybrid piezoelectric composites is governed by a multidimensional interplay between intrinsic material properties, interfacial polarization phenomena, connectivity architecture, and electromechanical coupling efficiency. Beyond simple phase combination, optimized hybrid systems require deliberate selection of matrix chemistry, ceramic filler characteristics, volume fraction, morphology, and interfacial engineering strategies to maximize the piezoelectric voltage coefficient (g_{33}), charge coefficient (d_{33}), dielectric permittivity (ε_r), and mechanical compliance simultaneously.

2.1. Polymer matrix selection and functional optimization

The polymer matrix serves multiple roles: mechanical compliance provider, dielectric medium, stress-transfer bridge, and polarization stabilizer. Among electroactive polymers, polyvinylidene fluoride (PVDF) remains the benchmark material due to its intrinsic ferroelectricity and relatively high piezoelectric coefficient for an organic system in β-phase-rich films (d_{33} ≈ 20–30 pC/N). PVDF crystallizes into five polymorphs (α, β, γ, δ, ε), with the all-trans β-phase being responsible for its highest spontaneous polarization [16]. Enhancement strategies reported in recent literature include:

- mechanical stretching to induce chain alignment;
- electrical poling under high fields;
- electrospinning-induced molecular orientation;

- incorporation of nucleating nanofillers;
- solvent engineering and controlled crystallization kinetics.

Phase-engineered PVDF systems have demonstrated significant improvements in dielectric constant and remnant polarization, thereby increasing energy density ($U \propto \varepsilon E^2 / 2$) [17].

Copolymer systems such as polyvinylidene fluoride-trifluoroethylene (PVDF-TrFE) offer superior ferroelectric ordering and reduced coercive field compared to PVDF homopolymer. The presence of TrFE units stabilizes the β-phase without requiring extensive post-processing. Thin-film PVDF-TrFE-based composites have demonstrated enhanced electromechanical coupling under low poling fields, which is advantageous for flexible and wearable energy harvesting systems [18]. Similarly, poly(vinylidene fluoride-co-hexafluoropropylene) (PVDF-HFP) copolymers introduce improved mechanical flexibility and toughness due to reduced crystallinity, while maintaining adequate dielectric response. Their lower modulus improves strain transfer from ambient vibrations, increasing the effective stress experienced by embedded ceramic phases [19].

Polyamides, with nylon being the most used, exhibit significant piezoelectric response among ferroelectric polymers. Notably, nylon stands out among piezoelectric polymers as a well-established material in the industry, having been used in clothing since the 1940s. The revelation of polyamides' piezoelectric properties occurred in 1969 by Kawai et al. [20]. Further exploration by Scheinbeim and Newman, particularly in odd-numbered nylons, uncovered enhanced piezoelectric properties due to the unique arrangement of amide groups, whereas in even-numbered polyamides dipole moments cancel each other out [21,22]. Nylon thus enables the development of piezoelectric fabrics. These fabrics can harness electric energy from movement, offering a sustainable power source for small electronic devices [23]. Nylon fabrics also find application in pressure sensing. However, challenges include the need for the δ-phase for piezoelectricity, which is not achieved through conventional fabrication methods like melt extrusion, and their hydrophilic nature, with water adsorption affecting their piezoelectric properties [24].

Among bio-based polymers, one polymer that has awakened strong interest is poly-L-lactic acid (PLLA), after reports of piezoelectricity without the need of poling [25]. This is an optically active polymer proposed for biomedical applications due to its ability to be resorbed and absorbed in the human body [26]. Piezoelectric response in PLLA is achieved when crystallites become oriented during fabrication process, most typically by cold drawing, associated with the polarity induced by carbonyl groups. This avoids the need of a further poling treatment, unlike PVDF and polyamides, simplifying the manufacturing of polymer-based piezoelectric devices. Indeed, applications in sensing and energy harvesting have already been proposed based on PLLA. Nonetheless, its piezoelectric coefficients (d_{14} ~10 pC/N), as other alternative polymers considered so far, are lower than best PVDF-based copolymers [27].

Piezoelectricity has been also observed in amorphous polymers, in which the absence of crystalline phases means that polarization is achieved as molecular dipoles become locked in place. Some of the most commonly used amorphous polymers are polyimide, polyvinylidene chloride (PVDC), and polyarylene ether nitrile (PAEN) [4].

Polyimides are characterized by exceptional thermal, mechanical and dielectric properties [28]. While PVDF exhibits superior piezoelectric characteristics, polyimides surpass PVDF in applications involving higher temperatures, maintaining their piezoelectric performance up to 150 °C compared to PVDF's degradation beyond 70–80 °C [29]. As amorphous polymers with a high glass transition temperature, polyimides employ a distinct piezoelectric mechanism from semi-crystalline polymers. The poling process involves subjecting the material to a high electric field at an elevated temperature to align the dipoles, followed by cooling below the glass temperature while maintaining the electric field [30]. This process aims to retain a partially polarized state at lower temperatures, making polyimides suitable for microelectromechanical systems (MEMS) devices, high-temperature tactile sensors and pyroelectric sensors, where PVDF and fluoropolymers lack stability [31]. Polyimides also find application in piezoelectric nanogenerators (PENG) for electronic skins or biomedical devices [28].

Recent studies emphasize that polymer dielectric constant critically influences the composite voltage output. Lower permittivity matrices enhance g_{33} (since $g_{33} = d_{33} / \varepsilon_r$), which is particularly important for vibration-based energy harvesters [32]. Therefore, matrix selection must balance dielectric screening effects and electromechanical conversion efficiency. Emerging elastomeric matrices such as polydimethylsiloxane (PDMS) have also been explored in architected 3–3 systems. Although intrinsically non-piezoelectric, their ultra-low modulus enhances mechanical amplification of ceramic skeleton deformation, substantially improving voltage output in structurally engineered composites [33]. Figure 1 shows a graded comparison of different polymer matrices used in composite piezoelectric structures.

To facilitate comparison among commonly used polymer matrices in ceramic–polymer piezoelectric composites, Table 3 summarizes their key dielectric, mechanical, and processing characteristics. Polymer matrices play a critical role in determining the flexibility, dielectric response, and interfacial compatibility of the composite system. Materials such as epoxy provide excellent struc-

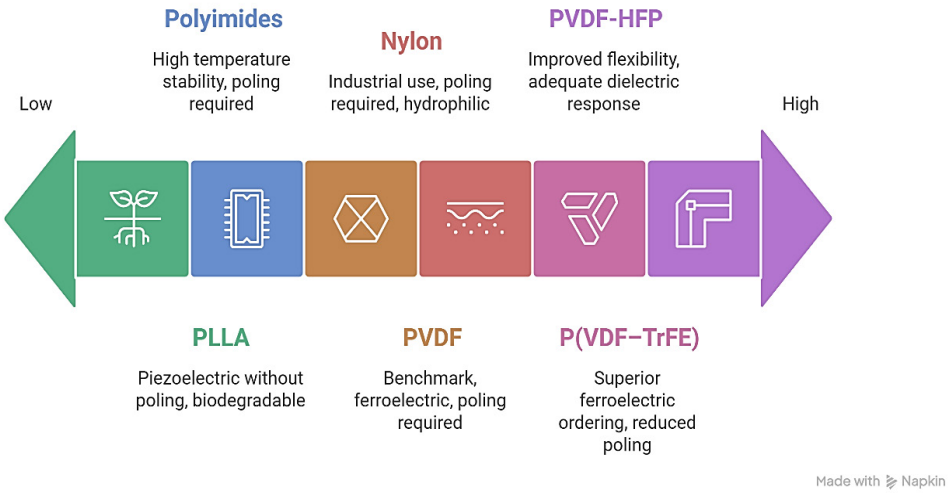

Fig. 1. Polymer matrices ranked by piezoelectric response and temperature stability.

Table 3. Key properties of commonly used polymer matrices for ceramic–polymer piezoelectric composites.

Polymer matrix	Dielectric constant (ε_r)	Young's modulus (GPa)	Typical processing method	Key advantages	Limitations
Epoxy	3–4	2–3	Casting, lamination, hot curing	Excellent mechanical strength, good adhesion to ceramic fillers, dimensional stability	Relatively brittle, limited flexibility
PDMS	2.5–3	0.001–0.003	Soft lithography, molding	High flexibility, stretchability, suitable for wearable devices	Low dielectric constant, weak mechanical stiffness
PVDF	8–12	3–3.5	Solution casting, electrospinning	Intrinsic piezoelectricity, good chemical resistance	Requires β-phase control for optimal performance
PVDF-TrFE	10–14	2–2.8	Spin coating, solvent casting	Strong ferroelectric and piezoelectric response	Higher cost and processing sensitivity
Polyimide (PI)	3–4	2.5–5.6	Thermal imidization, film processing	Excellent thermal stability and mechanical strength	More complex processing
Polyurethane (PU)	3–7	0.01–0.1	Solution casting, extrusion	High elasticity and durability	Lower thermal stability

tural rigidity and filler adhesion, while elastomeric matrices like PDMS and polyurethane offer superior flexibility suitable for wearable and deformable energy harvesting devices. Ferroelectric polymers including PVDF and its copolymers further contribute intrinsic piezoelectric activity, which can enhance the overall electromechanical response of the composite.

2.2. Ceramic filler selection, morphology control, and polarization efficiency

Ceramic inclusions constitute the primary active phase governing the intrinsic piezoelectric response of ceramic–polymer composites. Their crystallographic structure, spontaneous polarization, domain-wall mobility, and phase stability directly determine the achievable piezoelectric coefficients (d_{33}, g_{33}), electromechanical coupling factors, and dielectric permittivity of the overall system. Consequently, the selection of an appropriate ceramic phase requires a multidimensional optimization that balances functional performance with practical constraints.

Key trade-offs arise among (I) piezoelectric activity and dielectric constant, which influence charge generation and voltage output; (II) Curie temperature and thermal stability, which define the operational window; (III) environmental compliance, particularly in the case of lead-containing systems; (IV) processability, including sintering temperature, particle size control, and compatibility with low-temperature polymer processing routes; and (V) interfacial compatibility with the polymer matrix, which governs stress transfer efficiency and dielectric loss [34]. High-permittivity ceramics can enhance charge density but may also reduce voltage sensitivity (g_{33}) in composite configurations, while high ceramic loading improves electromechanical coupling yet increases stiffness and brittleness. Therefore, rational ceramic selection is

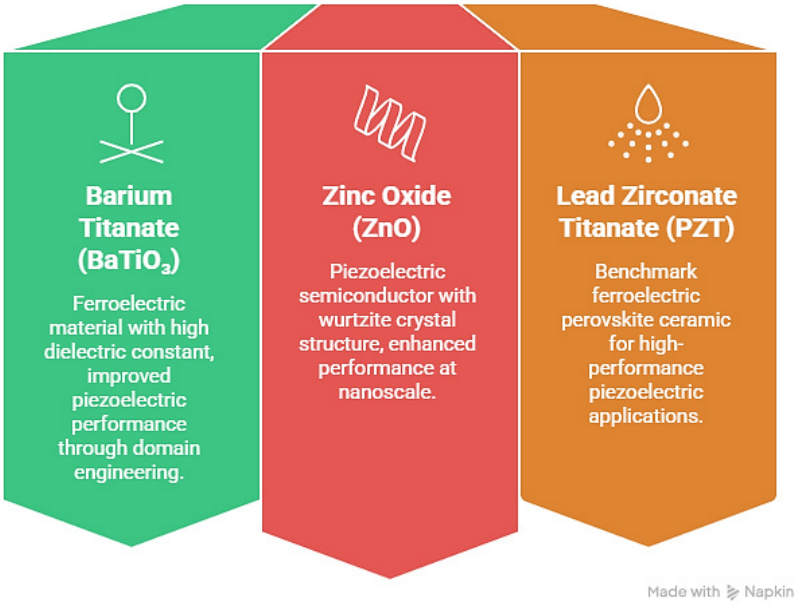

Fig. 2. Most well-known piezoelectric ceramic materials.

not solely based on intrinsic bulk properties but must also consider composite architecture, volume fraction, particle morphology, and interfacial engineering to achieve a targeted balance between energy conversion efficiency, mechanical flexibility, and long-term reliability [35]. Figure 2 is a comparison of three common examples of ceramic reinforcement phases in piezoelectric composites.

2.2.1. Barium titanate ($BaTiO_3$)

Barium titanate ($BaTiO_3$) was the first perovskite-structured ferroelectric material identified during World War II and initially attracted attention due to its high dielectric constant. Although its early applications were primarily dielectric rather than piezoelectric, substantial improvements in piezoelectric performance have been achieved through domain engineering and compositional modification, particularly via grain-size refinement and A/B-site substitutions [36]. For example, hydrothermally synthesized $BaTiO_3$ with controlled grain sizes of 1–2 μm has demonstrated d_{33} values up to ~ 460 pC/N, while Ca, Zr co-doped $BaTiO_3$ compositions have reported coefficients exceeding 600 pC/N, approaching those of soft PZT systems [37]. Nevertheless, the relatively low Curie temperature of $BaTiO_3$ restricts its operational temperature window, which may limit its use in high-temperature environments. In bulk tetragonal form, undoped $BaTiO_3$ typically exhibits moderate piezoelectric activity ($d_{33} \approx 60$–70 pC/N), yet at the nanoscale it shows pronounced size-dependent ferroelectricity; particle sizes in the range of 50–200 nm can preserve domain mobility while enabling improved dispersion in polymer matrices [38]. When incorporated into PVDF-based composites, $BaTiO_3$ significantly enhances dielectric permittivity and polarization under mechanical excitation. However, excessive ceramic loading (> 40 vol%) often results in agglomeration, increased brittleness, reduced flexibility, and interfacial charge trapping, thereby diminishing effective electromechanical conversion. To overcome these limitations, surface functionalization strategies—such as silane coupling agents or dopamine coatings—are widely employed to improve interfacial adhesion, stress transfer efficiency, and effective d_{33} [39].

Beyond $BaTiO_3$, Bi-containing perovskites have emerged as a major class of lead-free alternatives. The presence of highly polarizable Bi^{3+} cations with stereochemically active lone-pair electrons at the A-site enhances lattice distortion and polarizability, promoting strong electromechanical responses [40]. In particular, $Bi_{0.5}Na_{0.5}TiO_3$-based systems have demonstrated large strain responses and apparent piezoelectric coefficients exceeding 500 pC/N, often associated with field-induced phase transitions rather than purely intrinsic piezoelectric effects [41]. Similarly, $BiFeO_3$-based ceramics show enhanced d_{33} values due to electric-field-driven ordering of nanoscale domain structures. Importantly, Bi-containing perovskites exhibit favorable down-scaling behavior compared with many other lead-free systems, making them particularly attractive for miniaturized piezoelectric devices in microelectronic and energy harvesting applications [42].

2.2.2. Zinc oxide (ZnO)

Zinc oxide (ZnO) is a multifunctional piezoelectric semiconductor characterized by its non-centrosymmetric wurtzite crystal structure, which gives rise to intrinsic

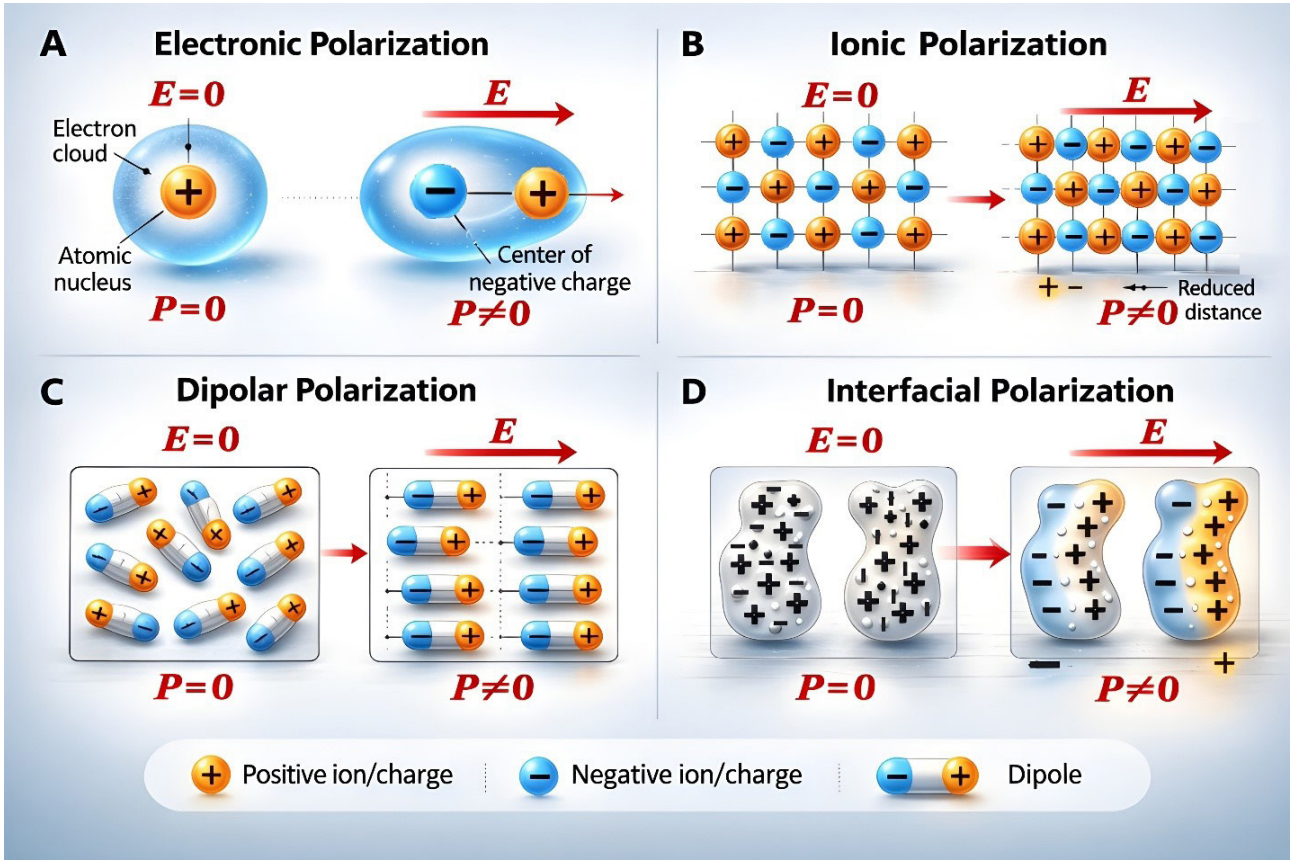

Fig. 3. Polarization mechanisms in dielectric and piezoelectric materials. Three-dimensional schematic illustration of four polarization mechanisms under an applied electric field E. (A) Electronic polarization results from the displacement of the electron cloud relative to the nucleus. (B) Ionic polarization arises from the relative displacement of positive and negative ions in the lattice. (C) Dipolar polarization occurs when permanent dipoles align with the electric field. (D) Interfacial polarization, also known as Maxwell–Wagner–Sillars (MWS) polarization, is caused by charge accumulation at interfaces between phases with different electrical properties and is particularly important in ceramic–polymer piezoelectric composites. Generated by the authors using Bio-Render®.

polarization along the c-axis. When engineered at the nanoscale, ZnO exhibits significantly enhanced electromechanical performance compared to its bulk counterpart. Nanorods and nanowires—typically with diameters in the range of 20–100 nm—can sustain higher elastic strain without fracture, leading to improved energy conversion efficiency, particularly under low-frequency mechanical excitation [43]. The effective piezoelectric constant is strongly dependent on morphology, aspect ratio, and crystallographic alignment; vertically aligned ZnO nanowires grown via vapor–liquid–solid (VLS) methods demonstrate higher effective piezoelectric coefficients than bulk ZnO due to reduced internal clamping and enhanced polarization along the growth direction [44].

In polymer-based composites (e.g., ZnO/PVDF systems), high-aspect-ratio nanostructures promote efficient stress transfer and interfacial polarization, while also introducing semiconducting functionality and biocompatibility—features advantageous for wearable and biomedical self-powered devices. Optimized and electrically aligned ZnO/PVDF composites have reported d_{33} values exceeding ~ 60 pC/N [45]. Furthermore, dielectric enhancement in such systems often surpasses classical rule-of-mixtures predictions due to interfacial Maxwell–Wagner–Sillars (MWS) polarization effects (Figure 3). Beyond piezoelectricity, ZnO fillers can impart photocatalytic activity, broadening functional integration potential. Representative demonstrations include ZnO nanorods grown on conductive textiles generating output voltages up to 1.8 V under mechanical excitation (~ 26 Hz), sufficient to power low-energy electronic components such as LCD displays [46]. Collectively, the synergy between nanoscale architecture, crystallographic orientation control, and interfacial engineering underpins the high performance of ZnO-based piezoelectric composites in next-generation energy harvesting systems.

2.2.3. Lead zirconate titanate (PZT)

Lead zirconate titanate (PZT) was first introduced in the early 1950s at the Tokyo Institute of Technology and remains the benchmark ferroelectric perovskite ceramic for high-performance piezoelectric applications [47]. Its outstanding electromechanical response (bulk d_{33} typical-

ly exceeding 300–500 pC/N, depending on composition and poling conditions) is fundamentally attributed to the presence of a monoclinic C_m phase at the morphotropic phase boundary (MPB) between the rhombohedral and tetragonal polymorphs, which enables polarization rotation and enhanced domain mobility [48]. In addition to its high piezoelectric coefficients and strong electromechanical coupling, PZT exhibits a relatively high Curie temperature (~ 350 °C), environmental stability, and broad technological applicability ranging from aerospace systems to precision microscopy [49]. Nevertheless, intrinsic ceramic brittleness and the presence of toxic lead remain critical limitations, particularly under increasingly stringent environmental regulations. To address these constraints while preserving performance, extensive research has focused on PZT-based composites, where nanoparticle-filled PZT/polymer systems have achieved d_{33} values approaching 90–100 pC/N at optimized ceramic loadings [50]. More recently, architecture connectivity designs—such as 1–3 and 3–3 composites and freeze-cast ceramic skeletons—have further improved energy harvesting efficiency by minimizing mechanical clamping, enhancing stress transfer pathways, and enabling controlled phase continuity [13,51]. In these engineered systems, the overall electromechanical performance arises from the synergistic interplay between intrinsic crystallographic phase behavior and mesoscale structural architecture [52].

Other ceramic fillers also used in polymer composites are aluminum nitride (AIN) or lithium niobate ($LiNbO_3$), among others [53,54]. The combination of ceramic fillers with piezoelectric polymers results in composites with improved thermal and electrical properties while retaining excellent mechanical characteristics. The size of ceramic particles allows the production of micro or nanocomposites tailored for specific applications. Processing conditions influence morphology and properties, with printing technologies enabling cost-effective production of large-area composite materials. Magnetoelectric composites, formed by blending piezoelectric polymers, such as PVDF and copolymers, with magnetic fillers like $Zn_{0.2}Mn_{0.8}Fe_2O_4$ (ZMFO) or $CoFe_2O_4$ (CFO), seamlessly integrate piezoelectric and magnetostrictive features. Also, the search of environmentally-friendly alternatives free of toxic elements like Ni and Co is playing an important role, ideally biocompatible. This dynamic synergy enables the manipulation of electrical polarization through magnetic fields and vice versa, resulting in a powerful magnetoelectric response. Ongoing research explores diverse applications for these composites, ranging from sensors, data memories, and energy collectors to biomedical devices, promising innovative solutions across various domains [55].

Ceramic fillers are the primary contributors to the intrinsic piezoelectric activity of ceramic–polymer composites. Their selection significantly influences the electromechanical coupling efficiency, dielectric response, and operational stability of the final composite material. Table 4 summarizes the key properties of representative piezoelectric ceramics commonly employed as fillers in hybrid composites. Among them, lead zirconate titanate (PZT) remains the benchmark material due to its exceptionally high piezoelectric coefficients and electromechanical coupling factors. However, increasing environmental concerns related to lead content have stimulated intensive research on lead-free alternatives such as barium titanate ($BaTiO_3$) and potassium sodium niobate (KNN). In addition, wide-bandgap materials including zinc oxide (ZnO) and aluminum nitride (AlN) have gained attention for micro- and nano-scale energy harvesting devices because of their excellent compatibility with thin-film processing and microfabrication technologies. Consequently, the choice of ceramic filler typically involves a balance between piezoelectric performance, environmental considerations, process compatibility, and mechanical integration within the polymer matrix.

Table 4. Key properties of representative ceramic fillers used in ceramic–polymer piezoelectric composites.

Ceramic filler	Crystal structure	Piezoelectric coefficient d_{33} (pC/N)	Dielectric constant (ε_r)	Curie temperature (°C)	Key advantages in composites
PZT	Perovskite	300–600	300–1200	~ 350	Very high piezoelectric response and electromechanical coupling
$BaTiO_3$	Perovskite	100–200	1200–1700	~ 120	Lead-free, good dielectric properties, widely studied
KNN	Perovskite	80–160	300–500	~ 420	Environmentally friendly lead-free alternative
ZnO	Wurtzite	10–15	8–10	non-ferroelectric	Easy nanostructure growth, compatible with flexible devices
AlN	Wurtzite	4–6	8–10	> 1000	Excellent thermal stability and compatibility with MEMS fabrication

3. COMPOSITE ARCHITECTURES AND PIEZOELECTRIC PERFORMANCE

3.1. Connectivity patterns

The piezoelectric performance of ceramic–polymer composites is fundamentally governed by phase connectivity, a concept first formalized in composite electromechanics theory to describe how active and passive phases interact mechanically and electrically. Connectivity determines stress transfer efficiency, electric field distribution, polarization continuity, dielectric response, and ultimately the effective electromechanical coupling factors of the composite system. In this article, we will examine the three most common design structures of piezoelectric composites (Figure 4).

In a **0–3 connectivity composite**, discrete piezoelectric ceramic particles are randomly dispersed within a continuous polymer matrix (e.g., PZT particles embedded in PVDF). This architecture is synthetically simple and mechanically flexible, making it attractive for wearable and low-modulus energy harvesters. However, because the ceramic inclusions are electrically and mechanically isolated, polarization continuity is interrupted and strain transfer is inefficient. The effective piezoelectric response is therefore strongly attenuated relative to bulk ceramics [3]. Experimental studies consistently report effective d_{33} values in the range of 50–150 pC/N for optimized 0–3 PZT/PVDF systems at moderate filler loadings, with performance strongly dependent on particle dispersion and interfacial bonding [56]. The response is typically limited by dielectric screening, interfacial charge trapping, and mechanical clamping imposed by the polymer matrix (Figure 5, top left).

In contrast, **1–3 connectivity composites** consist of continuous piezoelectric ceramic fibers or pillars embedded within a polymer matrix. A widely adopted fabrication route is the "dice-and-fill" technique, which creates a periodic array of vertically aligned ceramic rods subsequently infiltrated with polymer. This geometry establishes a continuous pathway for stress and polarization along the poling direction, significantly enhancing electromechanical conversion (Figure 5, top mid) [13]. Extensive experimental investigations demonstrate that 1–3 PZT/epoxy composites can achieve effective d_{33} values in the range of 300–500 pC/N, approaching bulk PZT ceramics ($d_{33} \approx$ 300–700 pC/N depending on composition and poling conditions). Moreover, thickness coupling factors (k_t) up to ~ 0.65–0.70 have been reported at ceramic volume fractions below 30%, exceeding those of many monolithic PZT ceramics ($k_t \approx$ 0.45–0.55) [60]. Finite element simulations confirm that stress is preferentially concentrated within the ceramic pillars while the polymer phase reduces lateral clamping, thereby enhancing effective longitudinal polarization.

An additional advantage of 1–3 composites is their reduced acoustic impedance relative to bulk ceramics, improving impedance matching to soft media such as water and biological tissue. This property has driven widespread adoption in ultrasonic transducers, hydrophones, and medical imaging systems [61].

Another important architecture is **3–3 connectivity**, in which both ceramic and polymer phases form continuous, interpenetrating three-dimensional networks. Such structures are often produced by fabricating a porous ceramic scaffold (e.g., via freeze casting or partial sintering) followed by polymer infiltration [62]. In 3–3 systems, the ceramic phase provides continuous polarization pathways while the polymer network contributes mechanical tough-

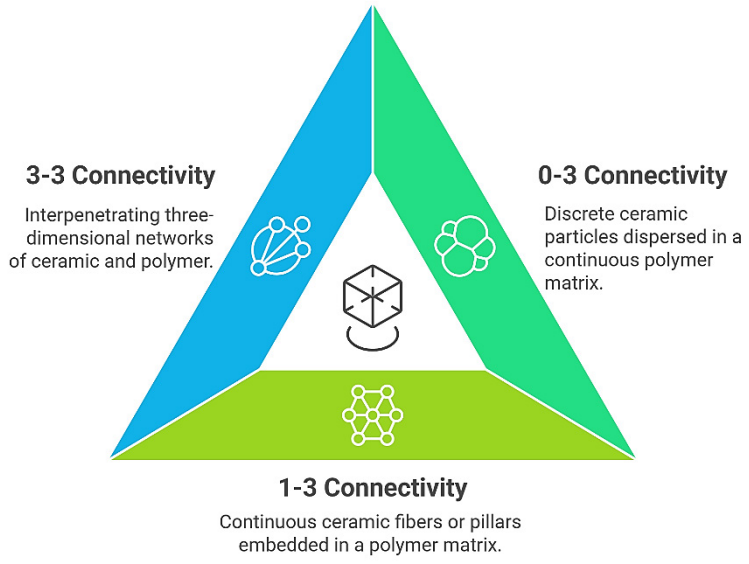

Fig. 4. Composites design systems.

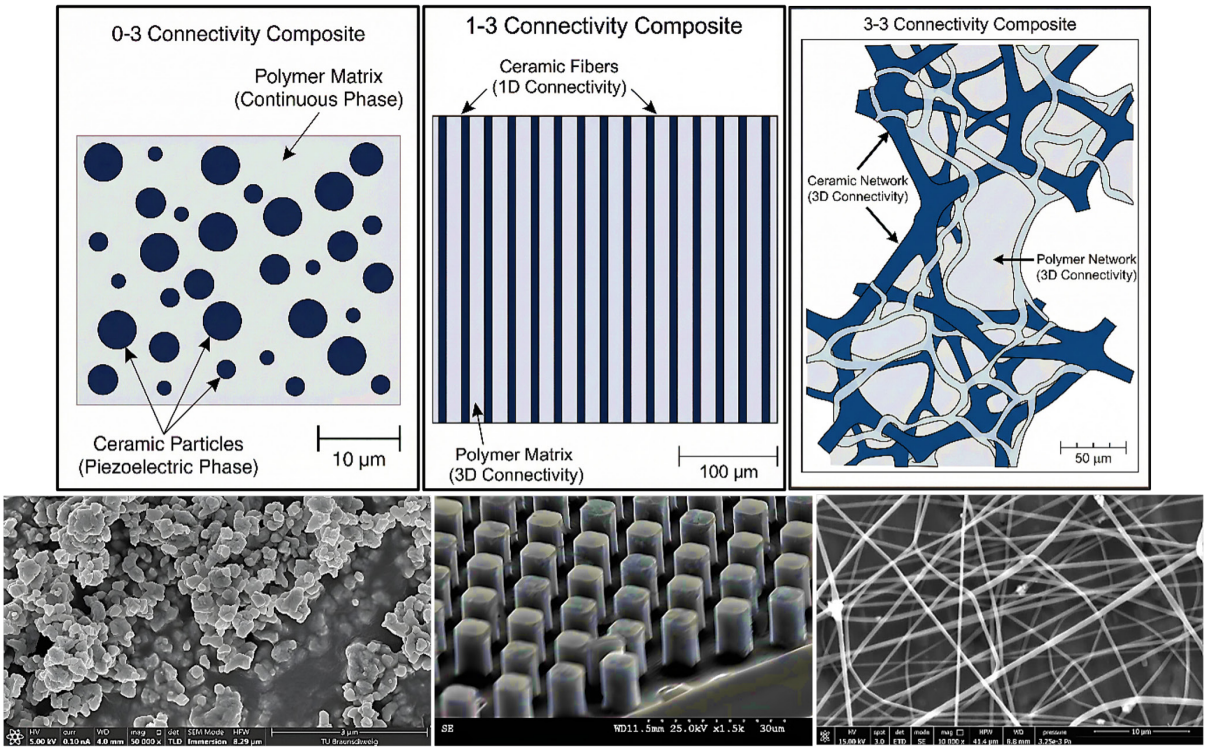

Fig. 5. Various architectural design systems for structural composites: (top left) 0-3, (top middle) 1–3 and (top right) 3–3 (generated by the authors using Bio-Render®). SEM micrographs: (bottom left) potassium–sodium niobate (KNN) piezoelectric ceramic with photopolymer resin "high-temperature V2" matrix in a 0–3 composite structure [57], (bottom middle) PDMS microhole arrays (cross-sectional and top views) replicated from the silicon micropillar master molds in a 1–3 composite structure [58] and (bottom right) PVDF nanofiber mesh with dispersed $BaTiO_3$ nanoparticles in a 3–3 composite design system [59]. Adapted from Refs. [57–59] under the terms of CC BY 4.0 license, © 2022 Mitkus et al., © 2020 Kashaninejad et al., © 2022 Magnani et al.

ness and flexibility. These composites exhibit improved strain accommodation and reduced brittleness compared to bulk ceramics. However, the complex multidirectional connectivity can reduce effective poling efficiency and increase dielectric heterogeneity, often leading to lower coupling factors compared with optimized 1–3 systems. Reported d_{33} values for 3–3 PZT/polymer composites typically range between 150–350 pC/N depending on ceramic fraction and scaffold morphology. Other connectivity types (2–2 laminar structures, 3–0 fully dense ceramic frameworks with isolated polymer inclusions, and emerging hybrid architectures) have been explored in modern energy applications; however, 0–3, 1–3, and 3–3 remain the dominant configurations in energy harvesting research (Figure 5, top right) [63].

3.2. Impact of connectivity on piezoelectric coefficients

Connectivity directly influences the effective piezoelectric coefficients (d_{33}, d_{31}), electromechanical coupling factors (k_{33}, k_t), dielectric permittivity, and mechanical quality factor (Q_m). Experimental comparisons consistently demonstrate that 1–3 composites outperform 0–3 systems in both longitudinal and transverse piezoelectric coefficients. For instance, a well-optimized 1–3 PZT/epoxy composite may exhibit:

- $d_{33} \approx 450$–500 pC/N;
- $d_{31} \approx -150$ to -250 pC/N.

In contrast, typical 0–3 PZT/PVDF composites report:

- $d_{33} \approx 80$–150 pC/N;
- $d_{31} \approx -50$ to -120 pC/N.

The superior performance of 1–3 systems arises from efficient axial strain transfer: deformation of the polymer matrix directly loads the continuous ceramic fibers along the poling direction, maximizing dipole reorientation and charge generation. In 0–3 systems, stress transfer is localized at particle–matrix interfaces, and internal electric field distribution is non-uniform, limiting effective polarization [60].

Mechanical quality factor (Q_m) and dielectric loss ($\tan\delta$) are also strongly architecture-dependent. 1–3 composites frequently exhibit higher Q_m and lower dielectric loss compared to 0–3 systems due to reduced interfacial polarization losses and better-defined domain alignment. These properties are particularly advantageous for resonant energy harvesting applications, where mechanical damping directly affects power density.

Nevertheless, trade-offs exist. Achieving high coupling in 1–3 composites often requires ceramic volume

Table 5. Comparison of (0–3), (1–3), and (3–3) ceramic–polymer composite architectures in terms of piezoelectric coefficients, coupling performance, and mechanical characteristics.

Composite type	Phase connectivity	Typical d_{33} (pC/N)	Typical d_{31} (pC/N)	Coupling factor k_{33}	Flexibility
0–3	Ceramic particles in polymer matrix	~ 100–150	~ –100 to –150	Low (≈ 0.2–0.3)	Very high (flexible)
1–3	Ceramic fibers in polymer matrix	~ 500	~ –200	High (≈ 0.6–0.7)	Moderate (stiff fibers)
3–3	Interpenetrating ceramic–polymer network	~ 200–300	~ –100	Moderate (≈ 0.3–0.5)	High (moderate stiffness)

fractions exceeding 40–60%, which reduces overall flexibility and increases fabrication complexity. In contrast, 0–3 composites maintain excellent mechanical compliance at low filler loadings (< 30 vol.%) but sacrifice piezoelectric output [13]. Thus, architecture selection must be application-driven:

- flexible wearable nanogenerators → typically favor 0–3 systems;
- ultrasonic and high-sensitivity transducers → favor 1–3 systems;
- mechanically robust multifunctional structures → explore 3–3 systems.

3.3. Enhanced piezoelectric coefficients via architectural optimization

Beyond classical connectivity definitions, recent studies demonstrate that geometric optimization within a given connectivity type can dramatically enhance performance. In 1–3 systems, parameters such as pillar aspect ratio, pillar spacing, diameter, and polymer modulus strongly influence effective coupling.

Modified 1–3 architectures with optimized pillar geometry and reduced lateral clamping have reported d_{33} values exceeding 700 pC/N under controlled conditions. Improvements are attributed to:

- enhanced poling uniformity;
- reduced transverse constraint;
- optimized electric field distribution;
- improved interfacial adhesion.

Finite element modeling confirms that increasing fiber aspect ratio enhances k_{33} up to a critical limit, beyond which mechanical instability (fiber buckling or fracture) degrades performance.

Emerging hybrid architectures—including graded 1–3+3 systems, partially connected ceramic networks, and bioinspired hierarchical scaffolds—have shown potential for further improving energy conversion efficiency while maintaining mechanical durability. Although still under development, such designs aim to decouple ceramic volume fraction from flexibility constraints, a longstanding limitation of conventional 1–3 composites.

The comparative data summarized in Table 5 highlight the strong dependence of effective piezoelectric performance on connectivity architecture, underscoring the necessity of structural design optimization alongside material selection.

It should be emphasized that although 1–3 connectivity architectures are capable of delivering near-ceramic-level piezoelectric coefficients and high electromechanical coupling, their performance is highly sensitive to geometric and compositional optimization. Fiber (pillar) diameter, aspect ratio, spacing, and volume fraction must be carefully engineered to minimize lateral clamping, ensure uniform poling, and prevent mechanical instability. Excessive ceramic loading—while beneficial for increasing d_{33} and k_{33}—can significantly reduce composite compliance, elevate acoustic impedance, and promote brittleness or microcrack formation under cyclic loading. Conversely, insufficient ceramic continuity compromises strain transfer efficiency and polarization coherence [61]. Therefore, optimal 1–3 composite design inherently involves balancing ceramic fraction with mechanical flexibility, dielectric behavior, and long-term durability. Overall, connectivity engineering remains a primary structural lever for tailoring ceramic–polymer piezoelectric composites to application-specific requirements: 0–3 architectures are well suited for lightweight and highly flexible devices, 1–3 systems enable high-sensitivity and high-output transducers, and 3–3 networks provide a compromise between mechanical robustness and electromechanical activity in multifunctional hybrid structures [13,51]. A summary of the systematic comparison of these design models is given in Table 5.

4. ADVANCED DESIGN STRATEGIES FOR ENHANCED PERFORMANCE

Recent progress in ceramic–polymer hybrid piezoelectric composites clearly demonstrates that architectural engineering—rather than simple compositional optimization—is the dominant factor governing electromechanical conversion efficiency. Modern design strategies increasingly focus on field distribution control, stress localization, interfacial polarization, and domain orientation to simultaneously enhance piezoelectric output, dielec-

tric strength, and mechanical robustness. The following subsections summarize three high-impact structural approaches supported by recent literature.

4.1. Heterostructured and multilayered architectures

Heterostructured and multilayered configurations represent a highly effective strategy for decoupling dielectric permittivity and breakdown strength—two parameters that are intrinsically coupled in single-phase materials. Recent studies on multilayer ceramic–polymer composites show that alternating ferroelectric-rich layers (e.g., $BaTiO_3$-, PZT-, or KNN-filled PVDF-TrFE) with low-loss polymer interlayers create strong interfacial polarization (MWS) effect, resulting in enhanced effective permittivity without sacrificing electrical reliability (Figure 6) [64].

In particular, heterolayered nanofiber systems combining PVDF-TrFE/$BaTiO_3$ composite fibers with conductive interlayers such as graphite nanosheets or reduced graphene oxide have demonstrated significant power density enhancement due to three coupled mechanisms [65]:

1. Stress redistribution and concentration at conductive interfaces, amplifying local strain in the active ferroelectric domains.
2. Interfacial polarization enhancement, increasing displacement current under dynamic loading.
3. Internal micro-capacitor effects, improving charge collection efficiency.

Such multilayered piezocomposites have achieved power densities exceeding 3 W/m^2 under low-frequency mechanical excitation in optimized configurations. Recent work in graded multilayer dielectric stacks further shows that compositional gradients (e.g., progressive ceramic loading across thickness) suppress local electric field concentration and delay dielectric breakdown, enabling higher operating voltages [66].

Theoretical modeling confirms that alternating high-permittivity ceramic-rich layers and mechanically compliant polymer layers produce a synergistic improvement in both dielectric constant (ε_r) and breakdown strength (E_b), thereby maximizing the energy harvesting figure of merit:

$$FOM \propto \frac{d^2 \varepsilon_r}{Y}, \quad (1)$$

where d is the piezoelectric coefficient and Y is Young's modulus. Multilayer design thus enables independent tuning of stiffness and electrical response—an outcome not achievable in homogeneous composites [67].

4.2. Three-dimensional hierarchical structures

Three-dimensional (3D) hierarchical architectures provide a multiscale approach to stress management and

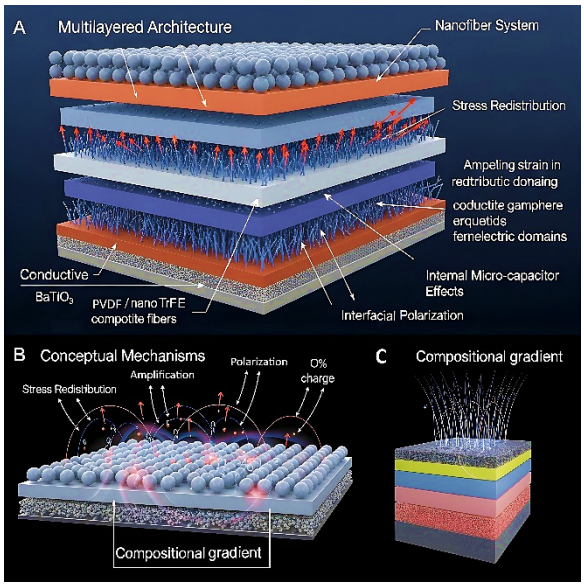

Fig. 6. Schematic of a functionally graded piezoelectric nanocomposite: (A) multilayer architecture, (B) polarization and charge-generation mechanisms, and (C) compositional gradient for enhanced energy-harvesting performance. Generated by the authors using QuillBot® Image.

charge generation. Electrospun nanofiber scaffolds with core–shell morphologies are particularly effective: ceramic-rich cores (e.g., $BaTiO_3$, PZT, or ZnO nanowires) provide strong intrinsic piezoelectric response, while polymer shells (PVDF, PVDF-TrFE, or PDMS) enhance mechanical durability and prevent dielectric failure. Hierarchical porosity within electrospun mats plays a critical functional role [68]:

- increases mechanical compliance for low-frequency deformation;
- enhances effective stress transfer to active ceramic domains;
- improves air permeability and biocompatibility for wearable systems.

Recent investigations demonstrate that 3D interconnected nanofiber networks increase surface-area-to-volume ratio and promote dipole alignment during in situ poling. Furthermore, templated 3D ceramic skeletons infiltrated with elastomeric polymers create stretchable composites with enhanced strain tolerance (> 20%) while preserving significant piezoelectric output [69].

The hierarchical integration of micro-scale ceramic frameworks with nano-scale fillers introduces dual-scale stress amplification. Finite element simulations confirm that hierarchical architectures create localized electric field intensification zones, thereby improving voltage output under weak mechanical stimuli typical of human motion (< 10 Hz). Such structures are especially advantageous in wearable, implantable, and textile-integrated energy harvesters where mechanical flexibility and high energy density must coexist [68].

4.3. Oriented fiber alignment and directional reinforcement

Directional alignment of dipoles, polymer chains, and ceramic inclusions is another critical architectural parameter governing anisotropic piezoelectric response. In semi-crystalline polymers such as PVDF and PVDF-TrFE, the piezoelectric β-phase (all-trans conformation) is the primary contributor to electromechanical coupling. Controlled electrospinning under high electric fields promotes in situ dipole alignment along the fiber axis, increasing β-phase fraction and enhancing d_{33} values beyond 60–70 pC/N in optimized nanofiber systems [70]. Key enhancement mechanisms include:

- electric-field-induced chain orientation during electrospinning;
- mechanical drawing and post-stretching, transforming non-polar α-phase into electroactive β and γ phases;
- thermal annealing under constraint, stabilizing crystalline orientation;
- dielectrophoretic alignment of ceramic nanowires, creating preferential 1–3 connectivity pathways within flexible matrices.

Aligned $BaTiO_3$ nanowires or PZT microfibers embedded in PVDF matrices have demonstrated significantly higher longitudinal piezoelectric coefficients compared to randomly dispersed systems, due to improved stress transfer efficiency and coherent polarization direction [71].

Advanced techniques such as magnetic-field-assisted alignment, 3D printing with shear-induced orientation, and electric-field-assisted assembly further enable spatially programmable anisotropy, allowing device designers to tailor energy harvesting response to specific loading modes (bending, compression, torsion) [72].

4.4. Integrated perspective

Collectively, heterostructured multilayers, hierarchical 3D architectures, and directional alignment strategies represent complementary pathways toward maximizing electromechanical conversion efficiency in ceramic–polymer hybrid piezoelectric composites. Rather than relying solely on increasing ceramic volume fraction—which often compromises flexibility and reliability—modern architectural engineering focuses on:

- interfacial polarization control;
- stress concentration management;
- dipole orientation optimization;
- multiscale structural synergy.

These strategies define the current frontier of high-performance piezoelectric energy harvesting materials and provide a rational framework for future development of lightweight, flexible, and high-output self-powered systems (Figure 7).

5. MICRO/NANO STRUCTURAL ENGINEERING

The progressive miniaturization of electronic systems has positioned micro/nano-piezoelectric energy harvesting (MPEH/NPEH) as a central research direction in the development of ceramic–polymer hybrid composites for enhanced energy harvesting. In this framework, micro–nano structural engineering serves as a key architectural strategy for optimizing electromechanical coupling and

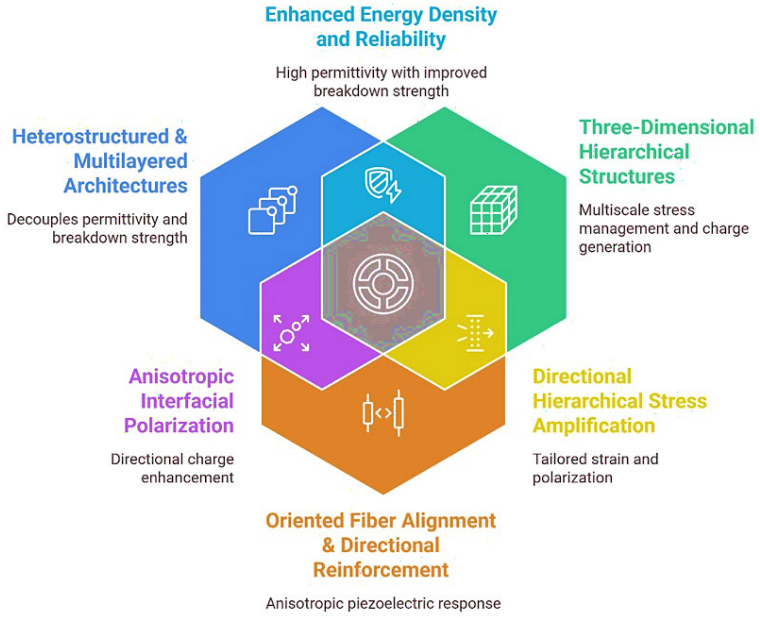

Fig. 7. Synergy in piezoelectric composite design.

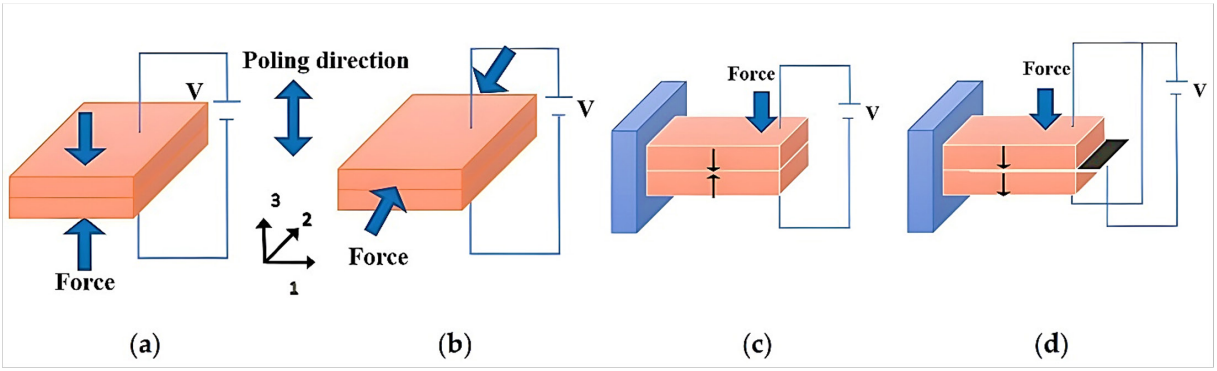

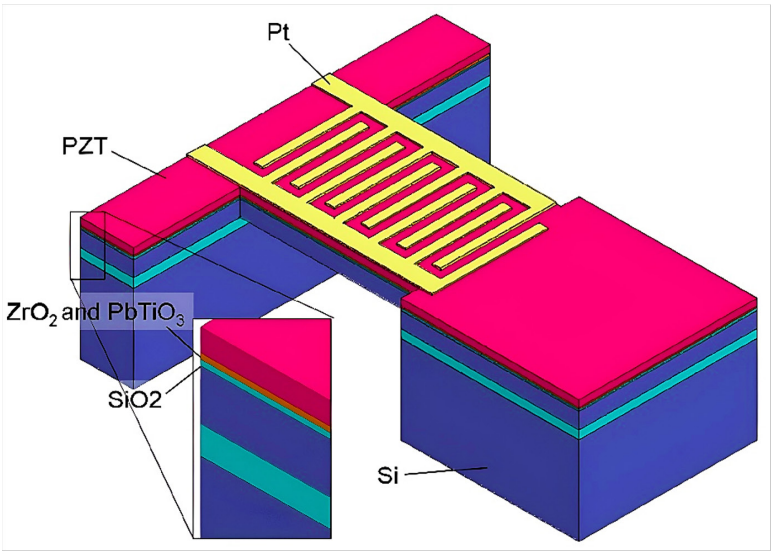

Fig. 8. Schematic structure of (top) d_{33} mode piezoelectric material operation (a), d_{31} mode piezoelectric material operation (b), PZT bimorph series operation (c), PZT bimorph parallel operation (d) [74] and (bottom) schematic drawing of the proposed piezoelectric MEMS energy harvester operating in the d_{33} mode for the purpose of scavenging low vibrations [76]. Adapted from Refs. [74,76] under the terms of CC BY 4.0 license, © 2020 Chilabi et al, © 2022 Zhou et al.

power output. At the microscale, controlled distribution and connectivity of ceramic phases (e.g., 0–3, 1–3, 3–3 architectures) regulate stress transfer efficiency, electric field distribution, and effective piezoelectric coefficients. Refinement of ceramic inclusions improves domain alignment and reduces structural defects, thereby enhancing intrinsic piezoelectric response. At the nanoscale, high-aspect-ratio nanofillers increase interfacial area and interfacial polarization (MWS) effect, leading to improved dielectric permittivity and local field amplification. Nanoscale confinement also influences domain wall mobility and dipole orientation, contributing to higher voltage output and power density. Hierarchical micro–nano architectures further promote stress concentration at active sites while maintaining mechanical flexibility, which is essential for low-frequency ambient excitation. However, performance gains must be balanced against dielectric loss, filler agglomeration, percolation effects, and mechanical embrittlement. Accordingly, precise control of dispersion, alignment, and interfacial bonding remains critical in the architectural optimization of hybrid piezoelectric composites for advanced energy harvesting applications.

5.1. Micro-piezoelectric energy harvesting (MPEH)

MPEH is a device combined with the MEMS technology, and this micro-processing technology is integrated with microsensors, micro-actuators, micro-electronic processing, and control unit structure in the micron scale (1 μm–1 mm). With the requirement of extremely low power electrical and MEMS devices, MPEH becomes more and more attractive. MPEH achieves the objective of miniaturization, which is always suitable for applying at high frequency corresponding to the high natural frequency. However, it is difficult to convert vibration energy into electricity in low-frequency environment. Therefore, among various structures combined with MEMS, cantilever MPEH has attracted much attention due to its lower structural stiffness, simple structure, easy to process and generate strain [73].

Figure 8(top) illustrates the fundamental electromechanical operating configurations of piezoelectric energy harvesters, including (a) the d_{33} mode under longitudinal polarization, (b) the d_{31} mode under transverse deformation, and (c–d) the series and parallel electrical connec-

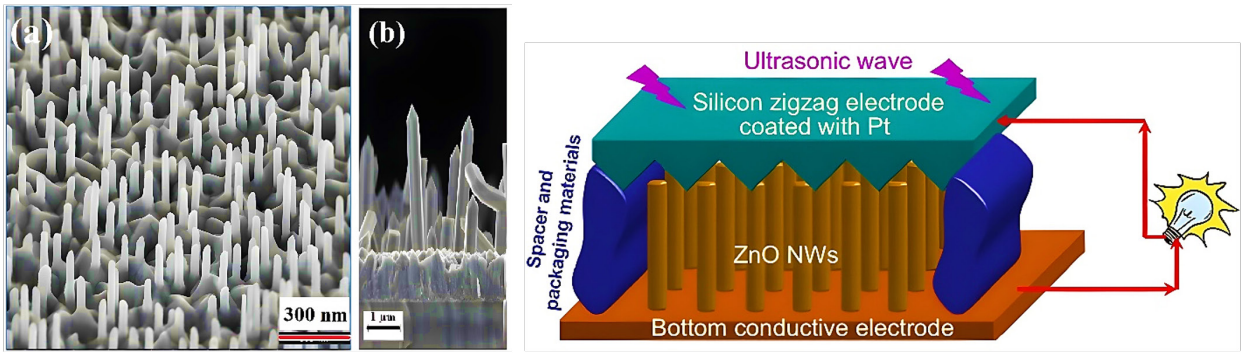

Fig. 9. (Left) Schematic diagram of (a) 40° tilted view SEM image of perpendicular ZnO NWs arrays grown on ZnO SL/Si (100) substrates at 10 mTorr and (b) deformed ZnO NWs arrays grown on ZnO/SL/Glass/ITO (ZnO nanorods on both silicon and glass-indium tin oxide) substrates at 5 mTorr [79]. (Right) A schematic diagram of a NW piezoelectric nanogenerator driven by an ultrasonic wave [80]. Adapted from Refs. [79,80] under the terms of CC BY 4.0 license, © 2020 ElZein et al., © 2021 Latif et al.

tions of PZT bimorph structures. These configurations are implemented in MPEH systems via top–bottom electrodes (TBEs) for d_{31} mode activation and interdigital electrodes (IDEs) for effective excitation of the d_{33} mode, enabling distinct strain–electric field coupling mechanisms and output characteristics. Notably, the d_{33} mode generally exhibits higher electromechanical coupling efficiency due to direct alignment of the electric field with the applied stress, whereas bimorph configurations in series and parallel provide design flexibility to tailor voltage and current output, respectively, for specific energy harvesting requirements [74].

In 2003, Sood et al. [75] successfully fabricated a MPEH (smaller than 300 × 300 μm) in d_{33} mode to store the electricity converted from high frequency sound energy, to provide electrical energy for minimize wireless sensor. The first layer of membrane (SiO_2 and/or SiN_x) can control stress and bow the cantilever structure; the second layer of diffusion barrier/buffer ZrO_2 prevented the electrical charge diffusion from the piezoelectric layer; the remaining upgrade layer is PZT piezoelectric materials, top interdigitate Pt/Ti electrode, respectively, as shown in Figure 8(bottom). The result showed that more than 1 μW power at 2.36 V DC was achieved [76]. A high Q_m ~ 800 of PZT thick film microcantilever was designed by Zhao et al. [77] using bulk silicon micromachining technology, which is potentially used for the mass detection and dynamic scanning force microscopy application.

5.2. Nano-piezoelectric energy harvesting (NPEH)

As it is known, piezoelectric nanowires can be stimulated by tiny physical movement and disturbance at the low frequency. The concept of nano-piezoelectric generator first addressed by Wang and Song [78] and expressed as the piezoelectric energy harvesting (PEH) in nano-structure often referred as nanogenerator (NG), which is the smallest power generation facility in the world. Figure 9(left) shows the structure of NG. It consists of piezoelectric zinc oxide nanowire (NW) arrays and converted the nanoscale mechanical energy to electric energy. The charge formation in semiconductor NW is derived from the bending NW by contacting atomic force tip as Schottky barrier, and then the output energy is transferred by conductive atomic force microscopy (AFM). Since then, many NG for selfpowered nanotechnology have sprung up [78].

In order to solve the problem of expensive equipment and complex operation of AFM systems, a nanogenerator (NG) was developed by integrating a Pt-coated serrated electrode with vertically aligned ZnO NWs to convert ultrasonic waves into electricity, as shown in Figure 9(right) [81]. The Pt coating NG enhanced the electrode conductivity and meanwhile created Schottky contact at the interface with ZnO, which needed much more stress to deform because of thickness of 1–3 mm. Maximum output energy was induced both with special substrate and an array of aligned ZnO/NWs.

As studied earlier, bulk-PEH mainly designed as cymbal or stacks is used under high stress and large power environment, such as road PEH, bridge PEH, etc. MPEH is always designed as cantilever structure due to its low frequency for vibration energy harvesting, while NPEH can be used for scavenging tiny and irregular vibration energy such as human motion and muscle contraction, which is potential for medical science with better biology compatible. However, there still existed many problems that should be overcome, such as naturally frequency, low efficiency, etc. Especially, despite both of MPEH/NPEH that realize the trends of miniaturization, however, there are still some new challenges brought. For MPEH, high working frequency and relatively low output power from piezoelectric film materials leads to the researching trend on the decrease of intrinsic frequency, integration of intermediate electrode, and performance of piezoelectric film to enhance the vibration energy harvesting in environment. For NPEH, it shows the disadvantages of high

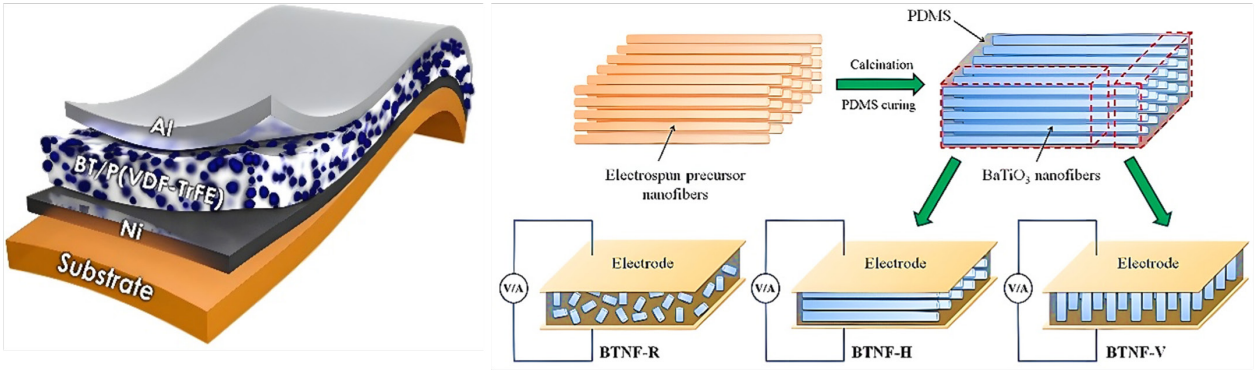

Fig. 10. (Left) Schematic of a PENG based on BT/PVDF-TrFE composites [82]. (Right) Schematic of fabrication procedure of NGs based on BT nanofibres in three kinds of alignment modes within PDMS with piezoelectric test circuits (output voltage changes of BT/PDMS p-NG under periodic mechanical compression) [88]. Adapted from Ref. [82] under the terms of CC BY 4.0 license, © 2021 Wang et al.; and Ref. [88] with permission, © 2016 American Chemical Society.

cost, complicated processing technology, poor stability of quantity production, and difficult to control assembly that hinders the practical application. Additionally, its limited output power introduces a new challenge to fabricate NG groups. Although there are many challenges before the practical application of NG, it is a valuable research area which is potential in biomedical, wireless communication and sensing fields.

6. NANO-COMPOSITE PIEZOELECTRIC MATERIALS

To avoid the relative brittleness of piezoelectric materials, a novel type of piezoelectric NG based on nanowire-polymer composite with relatively simpler fabrication processing was developed. It is made by the piezoelectric nanostructure embedded in polymer possessing both of high piezoelectric properties and flexibility. Basically, this device consists of four layers including top and bottom electrodes, the flexible substrate, and nanowire-composite layer, as shown in Figure 10(left) [83]. As BZT-BCT piezoelectric materials shows high piezoelectric constant, it has attracted much attention on NG area.

Wu et al. [84] synthesized lead-free BZT-BCT NWs and BZT-BCT/PDMS nanocomposite by the electrospinning method and applied it for high-performance flexible NG. It generated an output voltage, current, and power density of 3.25 V, 55 nA, and 338 mW/cm^3, respectively, which was larger enough to light commercial LCD. Due to the complicated composition and symmetry structure of BZT-BCT, it is difficult to synthesize BZT/BCT NWs via the hydrothermal method.

Recently, the $H_2Zr_{0.1}Ti_{0.9}O_3$ NWs with high aspect ratio acted as templates to converse a high-yield BZT-BCT NWs, which was fabricated via two-step hydrothermal methods by Sodano et al. [85]. The inverse piezoelectric constant of 90 pm/V, open circuit voltage, and power density of 6.25 V and 2.25 μW/cm^3 were obtained from BZT-BCT/PDMS nanocomposite NWs. However, the flexible NG device made by single BZT-BCT nano-piezoelectric material has relatively low output performance, which limits their use for operating commercial electronic devices. Then, the barium calcium zirconate titanate (BCZT) nanoparticles and Ag NWs were chosen as filler materials with PDMS matrix to fabricate a flexible NG, which effectively generated an output voltage peak of ~ 15 V and a current signal of ~ 0.8 μA without time-dependent degradation [86].

Wang et al. [87] fabricated a metal-insulator-metal structure NG composed of $(K_{0.48}Na_{0.52})(Nb_{0.95}Sb_{0.05})O_3$-$Bi_{0.5}(Na_{0.82}K_{0.18})_{0.5}ZrO_3$ nanofibers / PDMS nanocomposite with the ultrahigh inverse piezoelectric constant of 338 pm/V, and then the maximum output power of 0.5 μW and power density of 4.508 mW/cm^3 were obtained.

Until now, the orientation effect of nanowires or nanofibers from ferroelectric materials on piezoelectric properties has seldom been reported. Jeong et al. [88] manufactured a PDMS-based flexible nanocomposites including $BaTiO_3$ nanofibers with different alignment modes: aligned vertically, horizontally, or randomly in the PDMS matrix, as shown in Figure 10(right). The vertically aligned $BaTiO_3$ nanofibers achieved the highest output power of 0.1841 μW, maximum voltage of 2.67 V, and current of 261.40 nA, which was attributed to the vertical connection of nanofibers between electrodes compliant to mechanical stress. Table 6 summarizes the properties of piezoelectric NW materials applied in NG, mainly prepared by vapor liquid solid process, chemical epitaxial growth, and electrospinning technology. Compared with the bulk PEH, the processing technology of piezoelectric NW materials applied for NG is relatively complex and high cost, accompanied with the low piezoelectric properties. Consequently, researchers always utilize the output energy and output voltage for judging its performance, and the output power is between mW and μW. Although the output power from NG is relatively low, it can effectively harvest the tiny vibration in the environment. Thus,

Table 6. Properties of piezoelectric materials applied in NG.

Composition	Synthesis method	Output voltage (V)	Output energy (mW/cm^3)	Year
ZnO NW	Vapor liquid solid process	0.8×10^{-3}	10×10^{-6}	2020 [79]
PZT NWs	Chemical epitaxial growth	0.7	2.8	2009 [90]
PZT NWs	Electrospinning	6	200	2012 [91]
BZT-BCT NWs/PDMS nanocomposite	Electrospinning	3.25	338	2013 [84]
BZT-BCT NWs/PDMS nanocomposite	Hydrothermol	6.25	2.25×10^{-3}	2016 [85]
KNNS-BKZ nanofibers/PDMS	Electrospinning	10	4.508	2016 [87]

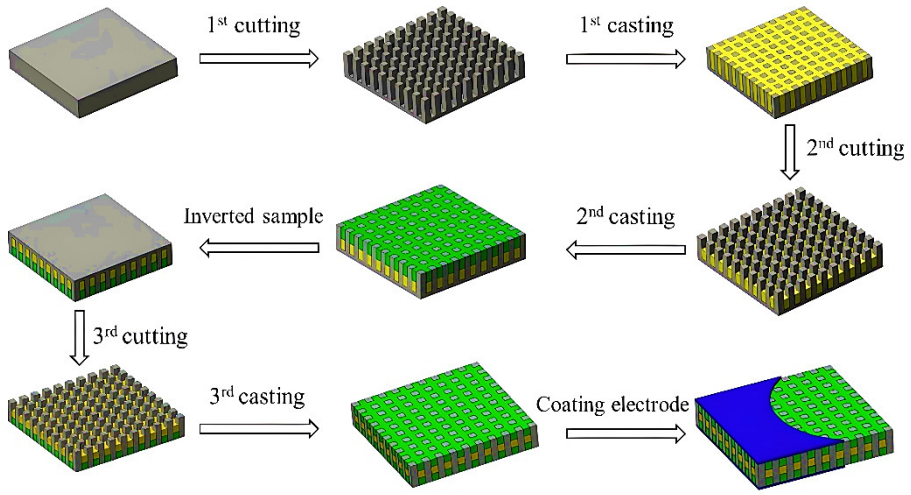

Fig. 11. Schematic diagram of preparation process of the novel composite by dice and fill method for manufacturing the 1–3 PZT/epoxy piezoelectric composite. Reproduced from Ref. [93] under the terms of CC BY 4.0 license, © 2020 Sun et al.

it is worthy to enhance the output power for NG which is potentially applied for biomedical and wireless sensor networks.

7. FABRICATION TECHNIQUES AND PROCESSING METHODS

7.1. Dice and fill method

Dice and fill fabrication remains the industrial benchmark for producing high-performance 1–3 piezoelectric composites. Originally introduced following the connectivity principles established by R.E. Newnham and co-workers [92], this subtractive approach enables the formation of highly ordered arrays of vertically aligned ceramic pillars embedded within a continuous polymer matrix. The process involves precision dicing of a dense piezoelectric ceramic plate—most commonly PZT—using a diamond saw to create orthogonal kerfs, followed by polymer infiltration and curing. The resulting architecture significantly reduces lateral clamping while preserving axial polarization continuity, thereby enhancing electromechanical coupling coefficients (k_t, k_{33}) and improving acoustic impedance matching (Figure 11) [93]. As extensively reported in foundational works by W.A. Smith and subsequent transducer studies [94], the ability to tailor pillar aspect ratio, kerf spacing, and ceramic volume fraction allows systematic optimization of d_{33} and bandwidth performance, which explains the continued dominance of this method in medical ultrasound and sonar systems.

Despite its structural precision and reproducibility, the dice-and-fill technique exhibits intrinsic scalability limitations. Because the method relies on mechanical micro-machining of brittle ceramics, it is susceptible to microcrack formation, edge chipping, and damage accumulation—particularly at fine pillar pitches below ~ 100 µm. The minimum achievable kerf width is constrained by blade thickness, leading to material waste and limiting geometric miniaturization. Furthermore, processing time and fabrication cost increase substantially for large-area devices, making the approach less economically favorable for distributed or flexible systems. As discussed in comprehensive transducer references such as those by Ahmad Safari, these constraints are acceptable in high-value precision applications but become critical barriers when transitioning toward scalable energy harvesting platforms [95].

From a techno-economic and industrial translation perspective, dice and fill is therefore best suited for small-area, high-performance devices requiring tight structural control and well-established reliability. However, emerging

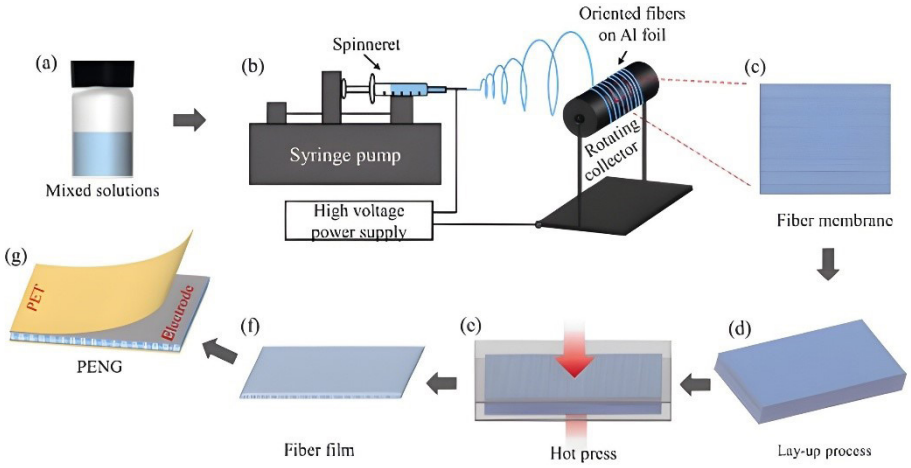

Fig. 12. Simplified overview of the elecrtospinning PENG process flow. Reproduced from Ref. [97] under the terms of CC BY 4.0 license, © 2025 Jalali et al.

applications such as wearable energy harvesters and conformal sensor networks demand fabrication routes compatible with large-area processing, geometric freedom, and potentially roll-to-roll manufacturing. In this context, architected approaches including freeze casting, additive manufacturing, and electrospinning offer enhanced design flexibility, albeit currently at lower manufacturing readiness levels. Consequently, while dice-and-fill remains the gold standard for structurally optimized 1–3 composites, its long-term relevance in next-generation scalable piezoelectric energy systems will depend on advances in precision micro-machining, kerfless structuring, or hybrid subtractive–additive manufacturing strategies [5].

7.2. Electrospinning and solution-based approaches

Electrospinning has emerged as the preeminent technique for fabricating piezoelectric composite nanofibers with precise morphological control and exceptional scalability [96]. This process utilizes electrostatic forces to draw thin polymer fibers directly from solutions containing dispersed ceramic nanoparticles, enabling continuous production of ultrafine fibers with diameters ranging from 100 nm to several micrometers. The versatility of electrospinning permits systematic variation of crucial processing parameters including applied voltage, tip-to-collector distance, polymer concentration, solvent composition, and flow rate, each of which profoundly influences the resulting nanofiber diameter, crystallinity, and piezoelectric properties (Figure 12) [98].

The electrospun PVDF nanofibers naturally tend toward the electroactive β-phase due to the intense electric fields during fiber formation, which directly align dipole moments along the fiber axis. This inherent phase preference eliminates the need for extensive post-fabrication poling treatments, substantially reducing processing time and equipment requirements. Studies quantifying the electrospinning parameter effects demonstrate that optimal conditions yield d_{33} coefficients of 51–65 pC/N for neat PVDF nanofibers, compared to approximately 25 pC/N for cast PVDF films [99].

Solution blow spinning represents an alternative production method offering comparable morphological control with enhanced scalability for high-throughput manufacturing. This technique combines compressed air injection with polymer solution atomization, enabling continuous fiber production without the high voltage requirements of electrospinning. The method shows particular promise for PVDF-based piezoelectric materials where solution parameters and air pressure optimization can achieve morphologies and performance characteristics rivaling those from conventional electrospinning [100].

7.3. Three-dimensional printing and additive manufacturing

Three-dimensional printing technologies have revolutionized composite design by enabling fabrication of complex geometries, graded compositions, and precisely controlled internal architectures impossible to achieve through conventional manufacturing [101]. Material extrusion-based approaches, including fused deposition modeling (FDM), permit direct printing of highly-filled polymer-ceramic suspensions, creating parts with tailored filler distributions and spatial control over composite properties [6]. The layer-by-layer deposition approach facilitates creation of precisely engineered multilayer structures where each layer composition can be systematically varied to achieve targeted property profiles (Figure 13).

Stereolithography and digital light processing (DLP) enable photopolymerization-based fabrication of piezoelectric composites with exceptional resolution and com-

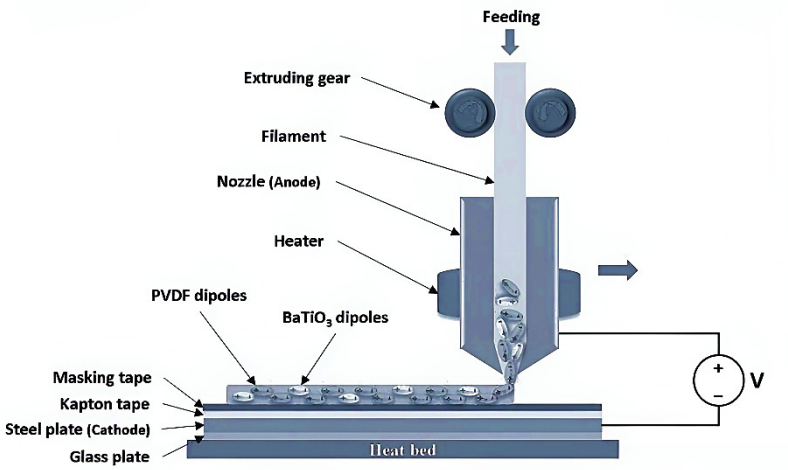

Fig. 13. Schematic of the in situ 3D printing and dipole alignment of PVDF and BTO filler. Reproduced with permission from Ref. [102], © 2017 WILEY-VCH Verlag GmbH & Co. KGaA, Weinheim.

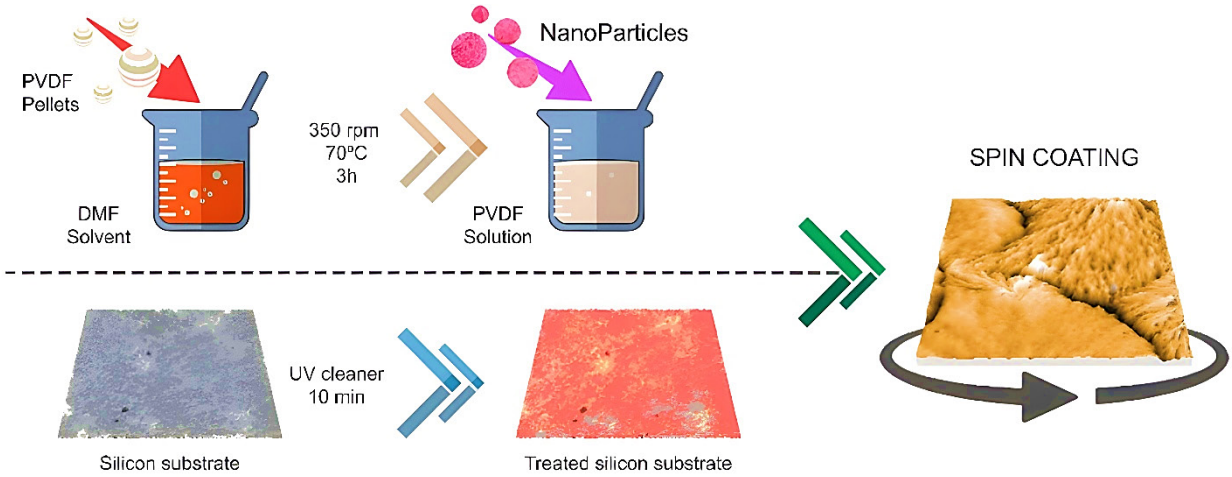

Fig. 14. Sketches of neat PVDF and hybrid PVDF–nanoparticle deposition on conductive pretreated substrates by spin coating technique. Reproduced from Ref. [107] under the terms of CC BY 4.0 license, © 2022 Nong et al.

plex internal structures [103]. These technologies excel at producing intricate lattice structures, hierarchical pores, and multimaterial interfaces with feature sizes approaching the micrometer scale. The photopolymerization process permits incorporation of photosensitive nanoparticle suspensions, enabling creation of composites with precisely positioned ceramic phases throughout the printed volume.

Recent advances in melt electrowriting have demonstrated the feasibility of printing mechanically enhanced polycaprolactone composites reinforced with functionalized titanate nanofiller, delivering Young's moduli exceeding 1.67 GPa—more than seven times higher than unfilled polymer controls [104]. The success of this approach stemmed from surface functionalization strategies that dramatically improved nanoparticle dispersion throughout the polymer matrix, preventing aggregation-induced mechanical weakness.

7.4. Nanoparticle dispersion and surface modification

Achieving uniform dispersion of ceramic nanoparticles throughout polymer matrices remains a critical technical challenge, as aggregated particles dramatically reduce effective reinforcement and electrical coupling [105]. Surface functionalization strategies employing silane coupling agents, surfactant coatings, and polymeric compatibilizers have demonstrated substantial improvements in nanoparticle-matrix interactions [106]. Trimethoxysilylpropyl methacrylate (TMSPM) functionalization significantly enhances the chemical linkage between ceramic nanoparticles and polymer chains, promoting effective local dipole-dipole interactions and substantially elevating the composite's remnant polarization (Figure 14) [108].

Comparative studies examining different functionalization approaches reveal that fluorinated surfactants establish more stable bonds with both polymer matrices

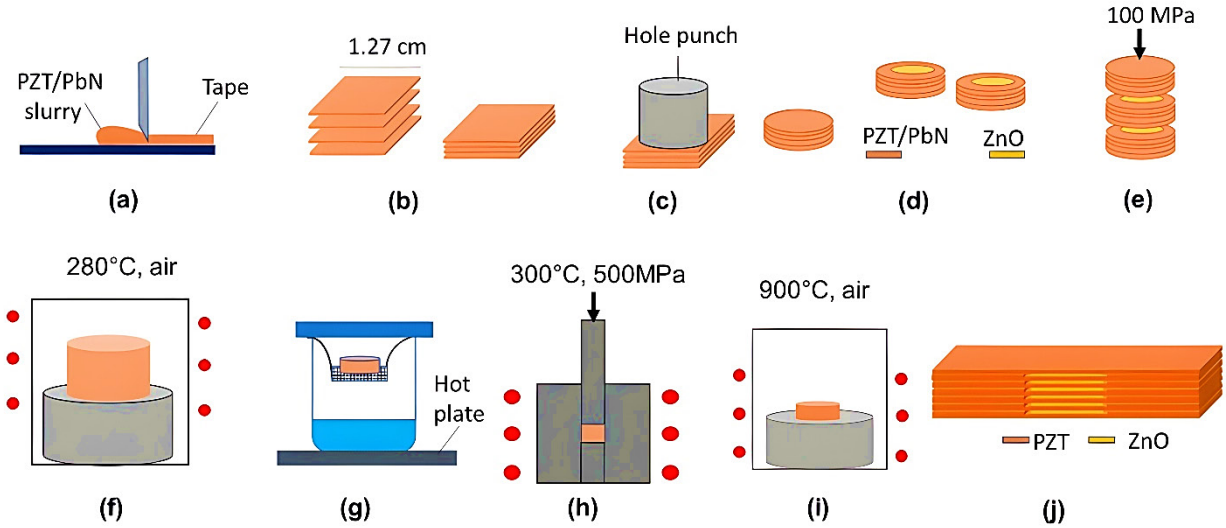

Fig. 15. Schematic illustration of the fabrication sequence for 0–3 PZT–sacrificial layer composites, including tape casting, sheet stacking and punching, concentric placement of the sacrificial layer, uniaxial lamination (100 MPa), binder burnout, steaming treatment, cold sintering, post-annealing, and final dicing to expose the sacrificial layers. Reproduced from Ref. [114] under the terms of CC BY 4.0 license. © 2021 Gupta et al.

and ceramic surfaces compared to conventional silane coupling agents [109]. The strategic selection of functional group chemistry permits fine-tuning of nanoparticle-matrix adhesion strength and interfacial polarization effects, directly translating to enhanced piezoelectric performance.

7.5. High and low-temperature processing

Fabrication techniques also differ in the temperature regime used. Conventional methods for PZT ceramics involve high-temperature sintering (e.g. 1100–1300 °C), which is incompatible with most polymers due to their thermal instability. To overcome this, researchers have developed low-temperature processing routes for piezoelectric composites [110]. One such method is cold sintering, where ceramics and composites are sintered at temperatures below 200 °C under high pressure (200–600 MPa). Cold sintering uses a liquid-phase sintering mechanism, often utilizing an additive that can form a transient liquid phase at low temperature, enabling densification without melting the polymer [111]. This technique has been applied to fabricate piezoelectric ceramic–polymer composites, including lead-free KNN and bismuth ferrite (BFO) ceramics, with high density and good piezoelectric properties at much lower temperatures. Cold sintering not only preserves the polymer matrix but also reduces energy consumption and environmental impact compared to conventional sintering [112]. Another low-temperature approach is polymer infiltration and pyrolysis (PIP), where a polymer is first infiltrated into a ceramic preform, followed by heating to pyrolyze the polymer and leave a ceramic structure. By controlling the polymer pyrolysis, one can create hierarchical structures (e.g. a polymer-derived ceramic with controlled porosity) that can then be used as the piezoelectric component. This method has been used to produce lead-free piezoelectric composites with a porous ceramic skeleton, which were then infiltrated with polymer to form the composite [113]. The hierarchical structures obtained from polymer pyrolysis exhibited improved flexibility and piezoelectric performance, as the polymer-derived ceramic had a fine microstructure that could be optimized for piezoelectricity (Figure 15).

Novel fabrication techniques and their impact on ceramic–polymer piezoelectric composites compared in Table 7. These methods enable greater control over composite structure and properties, ultimately leading to improved energy harvesting performance. Overall, the development of advanced fabrication techniques represents a central driver in the evolution of ceramic–polymer hybrid composites. By integrating emerging manufacturing approaches with innovative processing strategies, researchers can engineer precisely controlled micro- and macro-architectures that systematically optimize electromechanical coupling, mechanical compliance, and energy conversion efficiency. These advances not only enhance intrinsic material performance but also expand the design space for next-generation piezoelectric energy harvesters across biomedical, wearable, and structural monitoring applications. Furthermore, the ability to manipulate phase connectivity, interface quality, and porosity distribution at multiple length scales enables a more predictive structure–property relationship framework. Such architectural control facilitates the transition from empirical material optimization toward rational, application-driven composite design, thereby accelerating the translation of high-per-

Table 7. Key fabrication innovations. The table below summarizes some of the novel fabrication techniques and their impact on composite properties.

Fabrication technique	Description	Impact on composite properties	Ref.
3D printing	Layer-by-layer fabrication of polymer and ceramic components, enabling complex geometries and hierarchical structures.	Precise control over architecture; integration of multiple components; potential for tailored piezoelectric response.	[115]
Freeze-casting	Freezing a ceramic–polymer slurry to create a porous structure, followed by sublimation of ice to form a porous scaffold.	Highly ordered porosity; improved mechanical toughness and piezoelectric performance through strain accommodation.	[116]
Cold sintering	Low-temperature sintering (≤ 200 °C) under high pressure, enabling densification of ceramics without melting the polymer.	Preserves polymer; produces high-density composites with good piezoelectric properties at lower energy cost.	[111]
Polymer infiltration & pyrolysis	Polymer is infiltrated into a ceramic preform and then pyrolyzed to form a ceramic structure, which is infiltrated with polymer.	Creates hierarchical porous ceramics; improves flexibility and piezoelectric performance due to optimized microstructure.	[113]
Surface functionalization	Coating ceramic particles with polymer or coupling agents to enhance interface bonding.	Reduces interfacial defects; improves dispersion of ceramic; leads to more uniform strain transfer and higher piezoelectric response.	[7]
AC poling	Applying an alternating electric field during poling to improve domain alignment in composites.	Enhances effective piezoelectric coefficient d_{33} by ~ 30% compared to DC poling; reduces domain wall pinning and improves polarization efficiency.	[117]

formance piezoelectric systems from laboratory-scale prototypes to scalable technological platforms.

8. COMPARATIVE AND INTEGRATIVE ANALYSIS

The performance of ceramic–polymer hybrid piezoelectric composites cannot be fully understood through isolated parameter evaluation. Instead, energy-harvesting efficiency emerges from the coupled interaction between material selection, filler optimization, processing route, architectural configuration, and interfacial engineering. This section presents a comparative integrative analysis that systematically correlates these variables within a unified structure–process–property–application framework. By examining their combined influence rather than independent contributions, a hierarchical relationship among design parameters becomes evident, enabling identification of the dominant mechanisms governing electromechanical performance enhancement. The statistical analyses presented in Sections 8.1 and 8.2 were performed using a multivariate comparative approach based on quantitative data extracted from the reviewed literature. Data processing, correlation analysis, and graphical modeling were carried out using OriginPro® and MATLAB® to identify dominant trends and optimize fabrication and design parameters.

8.1. Multiscale analysis of the effect of essential parameters on piezoelectric properties

Figure 16 presents a comprehensive six-panel performance analysis of ceramic–polymer hybrid piezoelectric composites, integrating material comparison, fabrication scalability, filler-content optimization, architectural design effects, interface engineering, and application-specific performance metrics. This multi-dimensional evaluation indicates that architectural design strategies—particularly hierarchical structuring—serve as a dominant driver for synergistic enhancement of energy-harvesting performance when combined with optimized filler content, advanced fabrication routes, and tailored interface engineering.

The baseline material selection (Figure 16, top left) establishes the fundamental advantage of the hybrid approach. Pure PZT ceramic exhibits an exceptionally high piezoelectric coefficient ($d_{33} \approx 380$ pC/N) but negligible flexibility (score ≈ 5/100). In contrast, neat PVDF polymer offers outstanding flexibility (≈ 90/100) yet a low $d_{33} \approx 25$ pC/N. $BaTiO_3$ nanoparticles provide moderate ($d_{33} \approx 70$ pC/N) with poor flexibility. The resulting ceramic–polymer hybrid composite successfully merges these properties, achieving $d_{33} \approx 55$ pC/N while retaining a flexibility score of ≈ 85/100. This dual functionality constitutes the essential platform upon which subsequent architectural strategies are built; without it, even sophisticated designs would remain constrained by intrinsic trade-offs between piezoelectric response and mechanical compliance.

Fabrication technique selection (Figure 16, top right) further dictates the feasibility of implementing complex architectures. Electrospinning and 3D printing achieve the highest combined scores in scalability and processability (≈ 0.85–0.90), outperforming solution casting, hot pressing, and melt blending. These two techniques

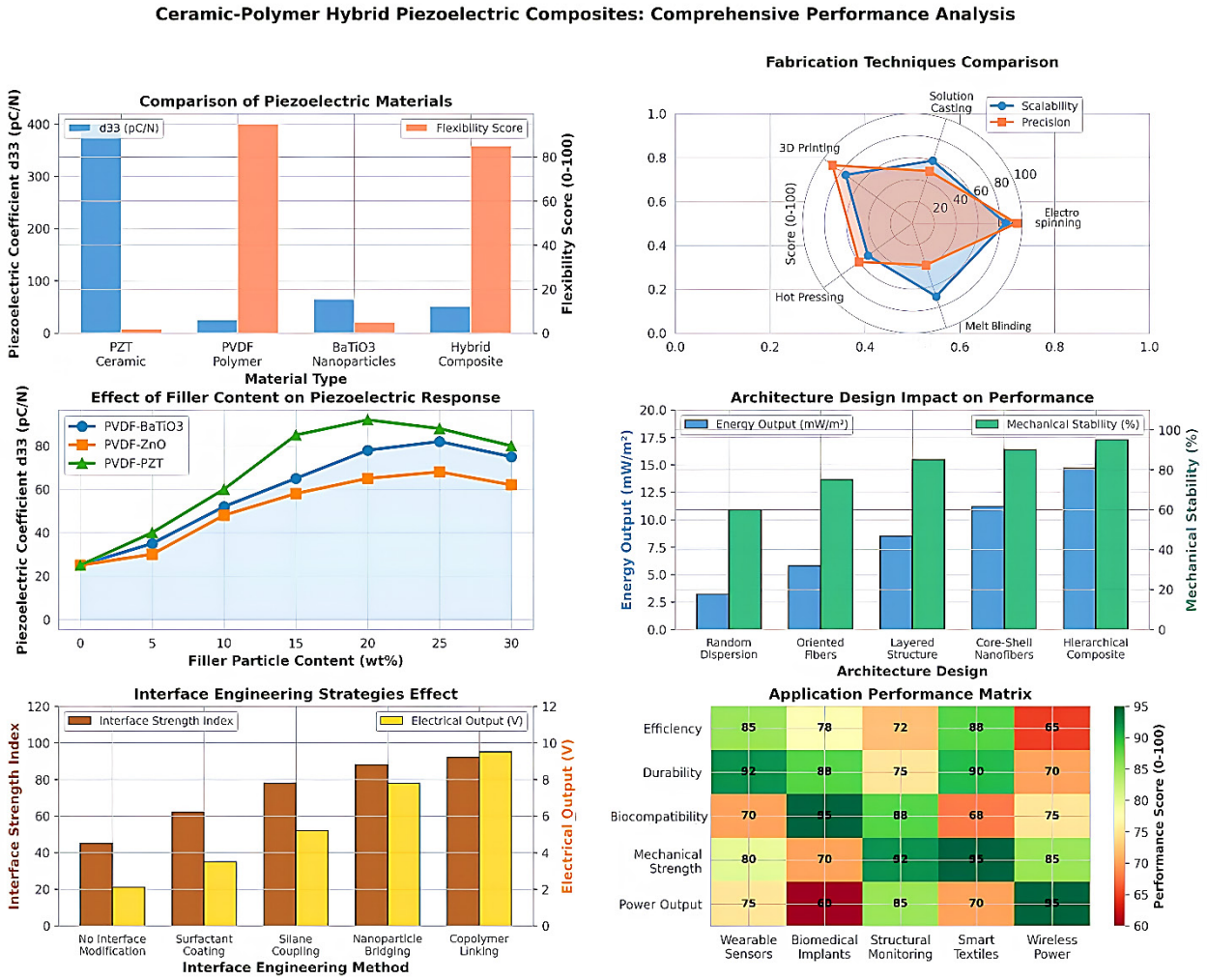

Fig. 16. Multi-parameter comparative statistical framework illustrating the coupled influence of material composition, fabrication strategy, filler concentration, architectural design, and interface engineering on energy-harvesting performance Developed analytical model by the authors with OriginPro® 2023.

uniquely enable precise alignment, controlled porosity, and multilayer deposition required for oriented-fiber and hierarchical architectures, thereby establishing a direct process–structure–performance relationship.

Optimization of filler particle content (Figure 16, middle left) reveals a consistent peak at ≈ 20 wt.% across all systems. PVDF–PZT reaches the highest d_{33} ≈ 75 pC/N, followed by PVDF–$BaTiO_3$ (≈ 70 pC/N) and PVDF–ZnO (≈ 65 pC/N). Beyond 20 wt.%, particle agglomeration, local stress concentration, and reduced polymer-chain mobility collectively contribute to a decline in piezoelectric response. This behavior suggests the presence of a percolation-assisted enhancement regime that is mechanically limited beyond the optimal concentration, identifying ≈ 20 wt.% as the effective design threshold for the architectures discussed below.

The core of the present study—architectural design impact—is quantified in Figure 16-middle right. Five representative architectures are compared in terms of energy output (mW/m^2) and mechanical stability (%). Random dispersion yields the lowest energy output (≈ 4 mW/m^2) and moderate stability (≈ 60 %). Oriented fibers improve performance to ≈ 6 mW/m^2 and 70% stability through dipole alignment. Layered structures further increase output to ≈ 9 mW/m^2 and 80% stability. Core–shell nanofibers achieve ≈ 12 mW/m^2 and 90% stability via enhanced interfacial polarization. The hierarchical composite architecture delivers the highest values: energy output ≈ 15 mW/m^2 (3.75-fold improvement over random dispersion) and mechanical stability ≈ 95%. These results strongly indicate that hierarchical organization maximizes stress-transfer efficiency, dipole alignment, and charge-collection pathways simultaneously, providing the dominant contribution to enhanced energy-harvesting performance.

Mechanistically, the superior behavior of hierarchical architectures can be attributed to multi-scale structural synergy. At the microscale, gradient filler distribution

promotes more uniform stress redistribution and mitigates local strain concentration. At the mesoscale, aligned pathways enhance dipole cooperativity and reduce dielectric screening effects. At the macroscale, interconnected conductive or semi-conductive networks shorten charge-collection distances and decrease internal resistance. This multi-level amplification of electromechanical coupling explains the substantial gain in energy output beyond what filler optimization alone can achieve.

Interface engineering strategies (Figure 16, bottom left) function as critical performance multipliers for the selected architectures. The copolymer-linking method achieves the highest interface strength index (≈ 90) and electrical output (≈ 10 V), followed by nanoparticle bridging (≈ 85, 8 V), silane coupling (≈ 75, 5 V), and surfactant coating (≈ 60, 4 V). No interface modification yields only ≈ 45 and 2 V, respectively. These findings indicate that robust interfacial bonding is essential for translating the theoretical advantages of hierarchical architecture into practical devices; without optimized interfaces, even advanced architectures may realize only 60–70% of their theoretical potential due to inefficient stress transfer and interfacial charge loss.

Finally, the application performance matrix (Figure 16, bottom righ) validates the practical relevance of the optimized hierarchical composite. The highest performance scores (> 90) are observed for wireless power and smart textiles, followed by structural monitoring (≈ 88–92) and wearable sensors (≈ 85–90). Biomedical implants maintain excellent biocompatibility (≈ 88–95) while achieving durability scores above 85. These results highlight that the combination of hierarchical architecture, 20 wt.% filler, electrospinning/3D printing fabrication, and copolymer interface engineering provides a versatile material platform suitable for high-efficiency energy harvesting across multiple demanding applications.

In summary, the six-panel analysis reveals a coherent synergistic hierarchy: the ceramic–polymer hybrid foundation supplies mechanical compliance and piezoelectric functionality; advanced fabrication routes enable structural precision; optimized filler content establishes the electromechanical baseline; hierarchical architecture delivers the largest performance amplification (≈ 3.75× energy output); and copolymer interface engineering maximizes stress transfer and charge continuity. When integrated, these elements increase energy output from 4 mW/m^2 to over 15 mW/m^2 while preserving flexibility, biocompatibility, and mechanical stability.

Nevertheless, further investigation is required to assess long-term electromechanical fatigue behavior, polarization stability under cyclic loading, and scalability of hierarchical fabrication for large-area devices.

Overall, the findings strongly support architectural design (particularly hierarchical structuring) as a pivotal strategy for next-generation flexible piezoelectric energy harvesters and provide a structured framework for rational, multi-parameter material optimization in future research.

8.2. Fabrication parameter and design optimization

To translate the connectivity architectural strategies established in Section 3.1 into high-performance devices, precise control of fabrication parameters and multilayer stacking is essential. Figure 17 provides a systematic optimization roadmap that directly underpins the superior energy-harvesting metrics of the ceramic–polymer hybrid composites. Electrospinning voltage optimization (Figure 17, top left) reveals a clear trade-off between fiber morphology and piezoelectric response. At 10 kV, coarse fibers (~ 850 nm) yield a modest d_{33} of ~ 35 pC/N. Increasing the voltage to the optimal 18 kV produces the thinnest fibers (~ 350 nm) and simultaneously maximizes the piezoelectric coefficient at ~ 62 pC/N. Beyond 18 kV, fiber diameter rebounds slightly and d_{33} declines, indicating that the 18 kV regime achieves ideal jet stretching, uniform ceramic nanoparticle alignment within the PVDF matrix, and maximal dipole orientation—conditions that are prerequisites for subsequent hierarchical layering.

The multilayer architecture effect (Figure 17, top right) quantifies the dramatic performance gains enabled by controlled stacking. A single-layer film delivers only ~ 150 MPa mechanical strength and ~3.5 (V) electrical output. Progressive addition of layers produces a near-linear improvement up to five layers, reaching peak values of ~ 390 MPa mechanical strength and ~ 14.5 V output voltage. Beyond five layers, marginal gains plateau and slight degradation appears at seven layers, attributable to cumulative interfacial defects and charge-trapping. These results demonstrate that the multilayer configuration—itself a foundational element of the hierarchical composite architecture—amplifies stress-transfer efficiency and inter-layer polarization synergy, delivering a fourfold enhancement in electrical output while simultaneously reinforcing mechanical integrity.

Poling process optimization (Figure 17, bottom left) highlights the critical temperature window for dipole alignment. Remnant polarization is highest (~ 14 μC/cm^2) at 60 °C but accompanied by elevated dielectric loss. As poling temperature rises, remnant polarization decreases sharply, reaching a minimum (~2.2 μC/cm^2) near 110 °C, while dielectric loss increases monotonically. The optimal compromise occurs at 100–110 °C, where remnant polarization remains sufficient (~ 3.5–4 μC/cm^2) and dielectric loss is minimized (~ 4.5%), ensuring low leakage and stable long-term performance. This refined poling protocol is particularly beneficial for multilayer and core–shell archi-

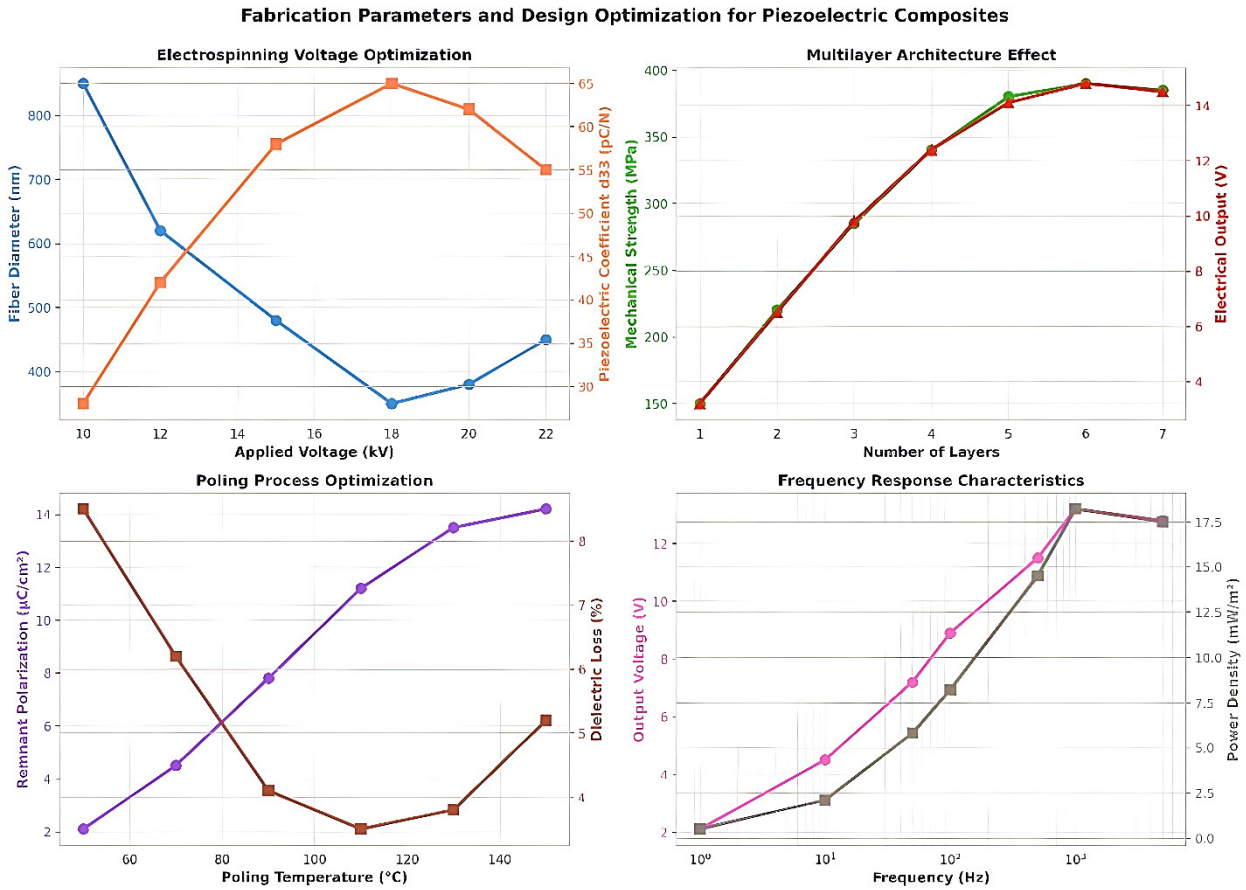

Fig. 17. The effect of design parameters, manufacturing, and additives on modifying piezoelectric properties Developed analytical model by the authors with OriginPro® 2023.

tectures, where uniform field distribution across multiple interfaces is essential.

Finally, the frequency response characteristics (Figure 17, bottom right) confirm the composite's suitability for real-world vibration energy harvesting. Both output voltage and power density increase steadily with frequency, attaining 13.2 V and 17.8 mW/m^2 at 1 kHz—values that represent more than sixfold improvement over low-frequency (1 Hz) operation. The absence of resonance peaks below 1 kHz and the broad-band response up to 10^3 Hz indicate that the optimized hierarchical multilayer structure efficiently couples mechanical stimuli across a wide frequency spectrum, a direct consequence of the refined fiber diameter, layer stacking, and poling conditions. Collectively, the optimized parameters—18 kV electrospinning, five-layer architecture, 100–110 °C poling, and operation near 1 kHz—act synergistically with the hierarchical design strategy. This integrated optimization elevates the baseline energy output from the random-dispersion architecture (≈ 4 mW/m^2) to > 15 mW/m^2 while preserving mechanical flexibility and long-term stability. The data in Figure 17 therefore provide not only process windows for reproducible fabrication but also mechanistic validation that architectural refinement, when coupled with precise parameter control, is the decisive pathway to next-generation flexible piezoelectric energy harvesters.

9. APPLICATIONS IN ADVANCED ENERGY HARVESTING AND SELF-POWERED SYSTEMS

9.1. Wearable and biomedical applications

Ceramic–polymer piezoelectric composites are widely implemented in wearable and implantable biomedical energy harvesters due to their flexibility and efficient electromechanical conversion from biomechanical sources such as gait, respiration, and arterial pulse [118]. For example, $BaTiO_3$/PVDF composites with high β-phase content and dispersed multi-walled carbon nanotubes (MWCNT) have been developed as flexible films for energy harvesting and localization applications, achieving enhanced mechanical sensitivity and electrical output under deformation typical of human motion [119]. Such composites enable continuous physiological sensing without external power supplies. Electrospun membranes comprising ZnO-based nanostructures embedded in PVDF demonstrate breathability, conformability, and superior voltage

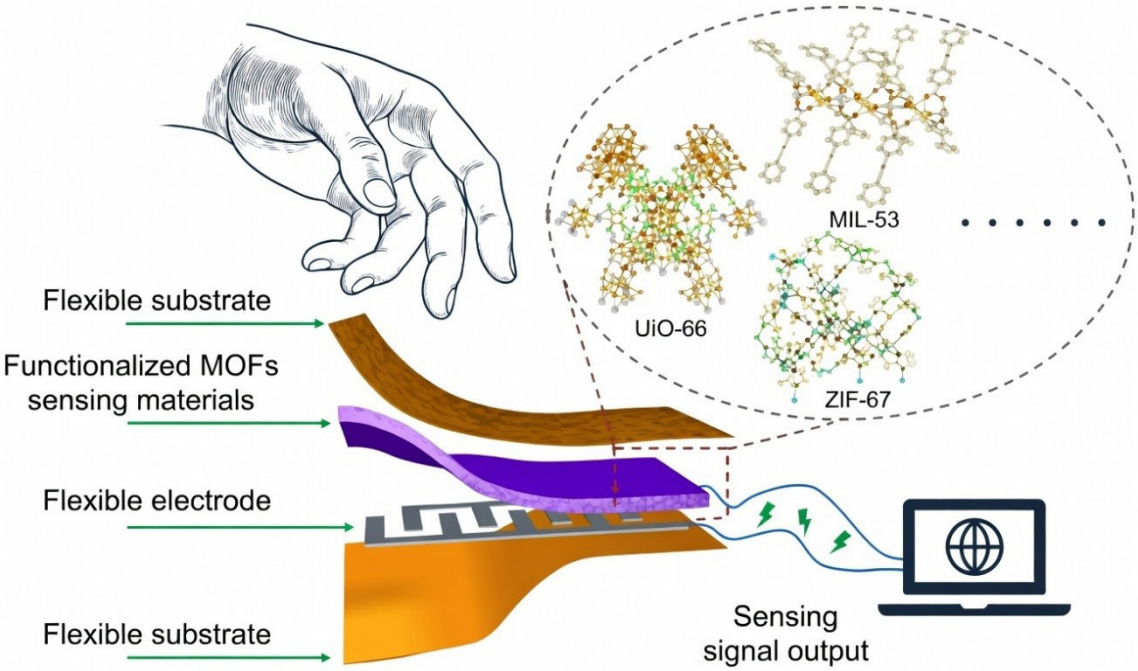

Fig. 18. Flexible piezoelectric energy harvesters leveraging functionalized MOFs (UiO-66, MIL-53, ZIF-67) for self-powered wearable sensing and mechanical-to-electrical conversion. Reproduced with permission from Ref. [121], © 2025 Wiley-VCH GmbH.

outputs (~ 20 V) under mechanical stress, making them suitable for wearable health-monitoring patches [120]. Additionally, advanced PVDF nanofibrous mats with metal-organic frameworks (MOFs) have been reported to harvest arterial pulse energy while exhibiting high sensitivity (~ 0.118 V/N), a promising approach for wearable biomedical sensors like the modern type of self-powered piezoelectric nanogenerator (PENG) (Figure 18) [122]. In implantable scenarios, lead-free piezoelectric fillers such as KNN or $BiFeO_3$ integrated with biocompatible polymers are emerging to address toxicity issues associated with traditional PZT ceramics.

9.2. Self-powered cardiac pacemakers

The possibility of harnessing the energy lost from a biological activity to provide energy for low-powered electronic devices has been also explored. Cardiac and lung motions serve as inexhaustible sources of energy during the lifespan. One of the first highlights in this area [123] is related with the use of an implantable physiological power supply using PVDF films. The prototype, that used the energy expended for breathing, was implanted in vivo on a mongrel dog and demonstrated a peak voltage of 18 V, which corresponds to a power of about 17 mW. Since then, there are several proposals for such devices that translate heartbeat vibrations into electrical energy using piezoelectric composites also for directly powering a cardiac pacemaker by harvesting the kinetic energy of heartbeat (Figure 19) [124]. Briefly, $Pb(Mg_{1/3}Nb_{2/3})O_3$-(28%)-$PbTiO_3$ (PMN-PT) was employed as piezoelectric layer and each side was sputtered with Cr/Au. A beryllium bronze foil was used to provide uniform stress distribution to the piezoelectric layer and then a PDMS film was deployed by spin-coating. To further improve the stability of the device and avoid potential erosion in the in vivo environment, a parylene film was deposited onto the PDMS film to form a compact and holefree coating layer. In vivo, a commercial cardiac pacemaker was directly powered by the implantable piezoelectric energy generator and monitored its behavior. It was concluded that patients do not need surgical replacement, or at least, the battery replacement will be less frequent. Currently, one of the most important application of energy harvesters is powering implantable biomedical devices [125].

9.3. Textile-based energy harvesting and smart clothing

Integration of piezoelectric composite fibers into textiles has created multifunctional platforms for wearable energy harvesting. Electrospun $BaTiO_3$/PVDF nanofibers and ZnO/PVDF composite yarns have been shown to generate sustainable electrical output from routine human motion (walking, running), providing power for embedded sensors or low-power electronics. Flexible composite fabrics incorporating ceramic fillers and polymer binders (e.g., PZT/PVDF-TrFE woven structures) demonstrate high mechanical endurance, air permeability, and consistent electrical output, supporting their use in smart garments and adaptive sportswear. These textile-based piezoelectric systems maintain comfort and wearability while harness-

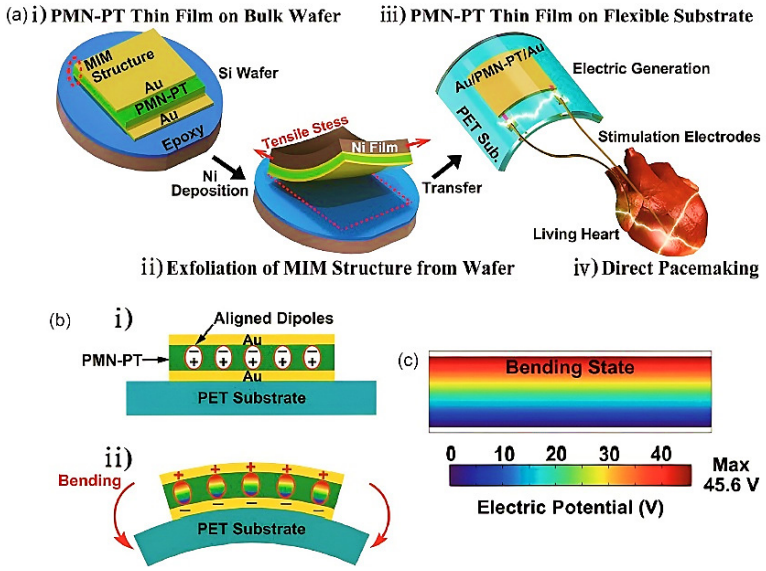

Fig. 19. (a) Schematic illustration of the fabrication process and biomedical application of the flexible PMN-PT piezoelectric energy harvester on PET substrate: (i) PMN-PT thin film deposited as MIM structure (Au/PMN-PT/Au) on bulk Si wafer with epoxy and Ni stressor layer; (ii) exfoliation/transfer of the MIM structure from the wafer using tensile stress; (iii) transferred flexible device (Au/PMN-PT/Au on PET) generating electricity under tensile/bending strain, with stimulation electrodes connected for direct pacemaking on a living heart; (iv) demonstration of self-powered direct cardiac pacemaking. (b) Piezoelectric generation mechanism in the flexible PMN-PT/PET thin film: (i) aligned dipoles in the unbent state; (ii) charge separation and electric potential generation upon bending. (c) Simulated piezoelectric potential distribution across the PMN-PT thin film under 0.36% tensile strain, showing maximum output up to 45.6 V. Reproduced from Ref. [80] under the terms of CC BY 4.0 license. © 2021 Latif et al.

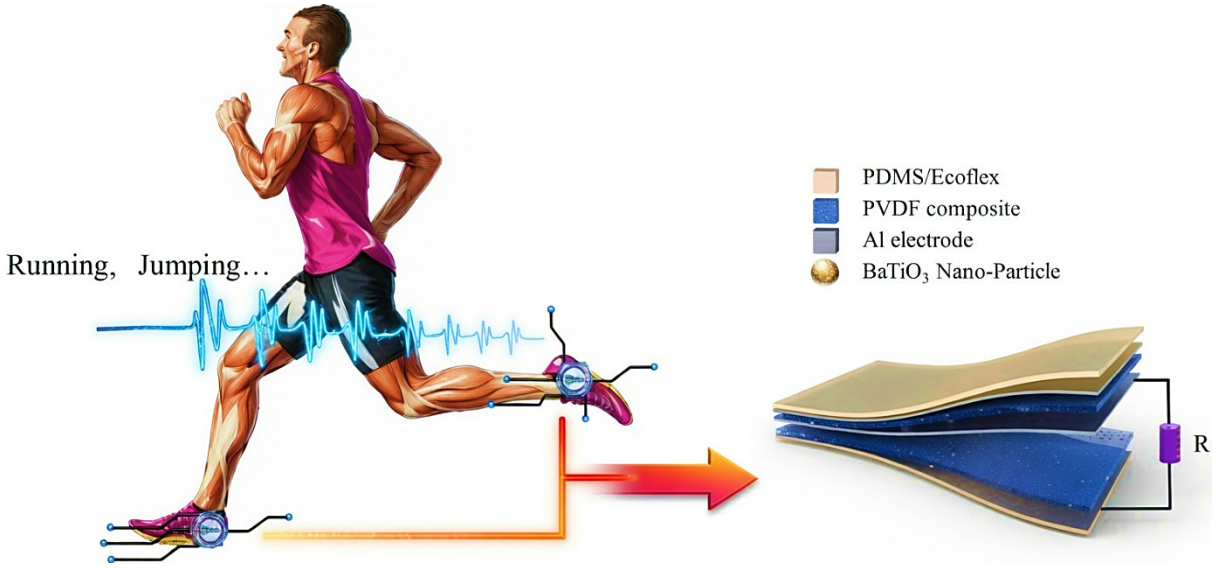

Fig. 20. A flexible multilayer $BaTiO_3$/PVDF–PDMS/Ecoflex hybrid nanogenerator textile attached to body joints harvests biomechanical energy during running and jumping, providing enhanced, stable output for self-powered motion sensing. Reproduced from Ref. [126] with permission, © 2025 American Chemical Society.

ing mechanical strain energy dissipated during ordinary activities, enabling decentralized self-powered sensing and data collection in smart clothing applications [126].

Furthermore, advanced textile fabrication methods such as multilayer weaving and conductive coatings improve the mechanical durability and electrical stability of piezoelectric fabrics under repeated deformation and washing. Hierarchical and aligned fiber structures enhance stress transfer and electromechanical conversion efficiency (Figure 20). In addition, hybrid textile systems integrating piezoelectric fibers with flexible energy-storage elements enable more stable and continuous power supply for wearable electronics, supporting the development of reliable self-powered smart garments [128].

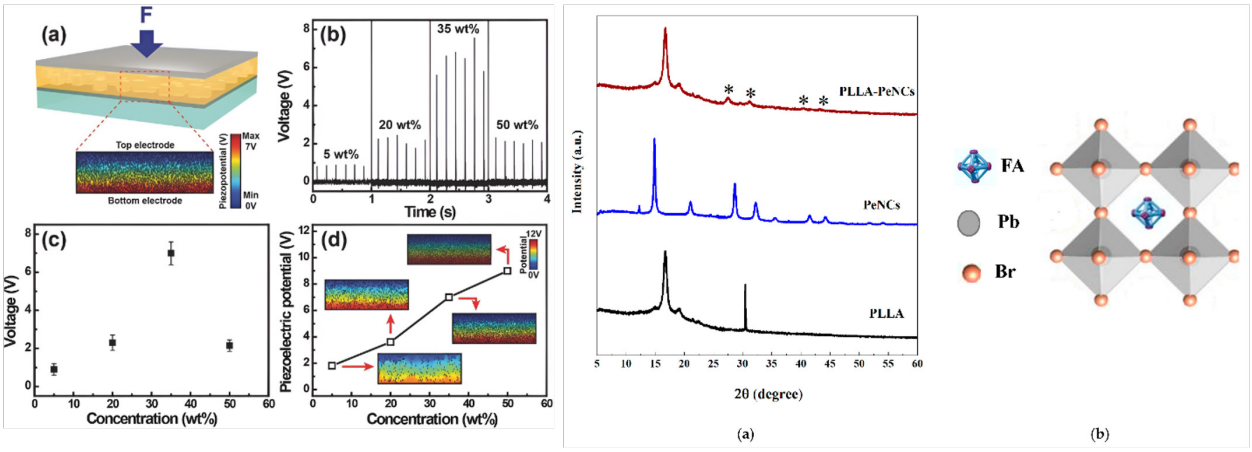

Fig. 21. (Left) (a) COMSOL® simulation model of a nanogenerator. The simulated piezoelectric potential distribution inside the composite between top and bottom electrodes is indicated by color code. (b) Output voltage from nanogenerators with different $FAPbBr_3$ nanoparticles concentration. (c) The variation of output voltage with different $FAPbBr_3$ nanoparticles concentration. (d) COMSOL® simulation result of output potential distribution of the nanogenerator with different $FAPbBr_3$ nanoparticles concentration [134]. (Right) (a) X-ray diffraction pattern of pure $FAPbBr_3$ NCs, PLLA, and PeNCs–PLLA nanofibres; * indicates the peaks belonging to $FAPbBr_3$. (b) The cubic crystal structure of $FAPbBr_3$ NCs at room temperature [135]. Adapted from Ref. [134] with permission, © 2016 WILEY-VCH Verlag GmbH & Co. KGaA, Weinheim; and from Ref. [135] under the terms of CC BY 4.0 license, © 2023 Tabassum et al.

9.4. Self-charging sport-activity electronics systems

Piezoelectric transduction is an approach that has received attention in the area of elecromechanical energy harvesting, i.e., the generation of electrical energy from mechanical vibrations [129]. ZnO nanowires [78], lead zirconate titanite (PZT) nanofibers [130], barium titanate ($BaTiO_3$) [131] and PVDF [132] are examples of piezoelectric materials that have been used to construct nanogenerators and to effectively power small electronic devices, such as lighting up LEDs [133]. In this context, formamidinium lead bromide ($FAPbBr_3$) nanoparticles (polycrystalline formamidinium lead bromide / cubic perovskite structure) uniformly mixed with polydimethylsiloxane (PDMS) and then spin-coated onto an indium tin oxide (ITO)-coated polyethylene terephthalate (PET) substrate and integrated with Al, demonstrate a high performance as energy harvesting devices. The $FAPbBr_3$-PDMS composite generates electric potential under an external stress with output voltage and current density of 8.5 V and 3.8 μA/cm^2, respectively, the nanoparticles serving as the energy generation sources as shown in Figure 21. The generated energy can be used to charge a capacitor and light up a LED through a bridge rectifier [134].

A primary motivation for self-charging structures is to use them for powering small electronic components. Piezoelectric shoes, electronic skin and other energy harvesting devices have been developed to take advantage of the produced vibration from human body activities such as: walking, running, breathing, and dancing to power-up low power electronic devices (Figure 22). In addition, large-scale human-motion energy harvesting concepts have been proposed, such as piezoelectric or transparent floor panels integrated into dance clubs, where the mechanical impacts generated by dancing participants are converted into electrical energy. A representative example is the human-powered generation system proposed by Paulides et al. [136], in which electrical power is harvested from the motion of dancers, demonstrating the feasibility of utilizing collective human activity as a sustainable energy source [136].

Overall, the integration of piezoelectric materials into self-charging sport-activity electronic systems represents a promising pathway toward sustainable and maintenance-free power sources for wearable and portable devices. Continued advancements in material engineering, device architecture, and energy management circuits are expected to further enhance power density, mechanical durability, and conversion efficiency. In particular, the development of flexible and hybrid piezoelectric composites will play a critical role in enabling seamless integration with human-centric applications, thereby accelerating the transition toward autonomous, energy-self-sufficient electronic systems.

10. CURRENT CHALLENGES, FUTURE PERSPECTIVES, AND RESEARCH DIRECTIONS

Polymer–ceramic piezoelectric composites for energy harvesting have shown significant potential; however, several challenges remain for their widespread implementation. Key issues include achieving uniform dispersion of ceramic fillers within polymer matrices, improving interfacial compatibility, and enhancing long-term mechanical and electrical stability under cyclic loading. Fu-

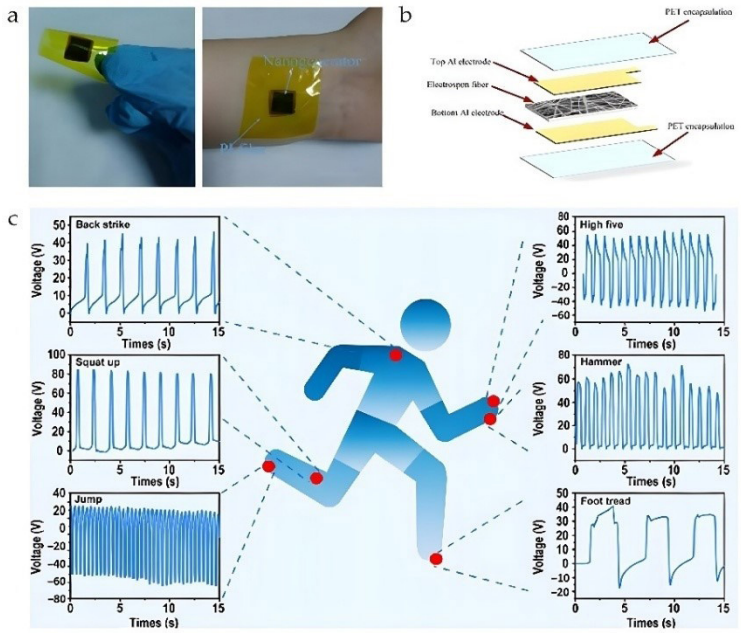

Fig. 22. (a) Flexible nanogenerator with piezoelectric layer/friction layer. (b) Environmentally friendly nanogenerator with PVDF/BZT composite material. (c) Voltage signal test results of PVDF/BTO at different wearing positions. Reproduced from Ref. [137] under the terms of CC BY 4.0 license. © 2024 Zhang et al.

ture research is expected to focus on optimizing composite architectures, developing scalable and cost-effective fabrication techniques, and improving electromechanical conversion efficiency. In addition, the integration of these composites into flexible and miniaturized devices will play an important role in advancing practical self-powered energy-harvesting systems (Figure 23). In the following discussion, we will further explore some of the most important challenges.

10.1. Performance degradation and long-term stability

Despite remarkable progress, piezoelectric composites exhibit gradual performance degradation during extended operation due to mechanical fatigue, moisture absorption, and interfacial delamination [37]. The polymer matrix's susceptibility to environmental moisture and thermal fluctuations can compromise both mechanical and electrical properties. Future research must develop enhanced environmental protection strategies including improved encapsulation materials and hydrophobic surface treatments that preserve functionality during prolonged exposure to humid environments and body fluids.

10.2. Manufacturing scale-up and cost reduction

Current fabrication approaches such as electrospinning, while producing exceptional material properties, suffer from limited production throughput—typically 1–10 grams per hour—rendering large-scale commercialization economically challenging [41]. Development of roll-to-roll electrospinning systems and continuous solution blow spinning methods shows promise for achieving industrial production rates while maintaining quality specifications [21]. Investment in automated 3D printing systems specifically designed for piezoelectric composite production may provide viable alternatives for localized manufacturing and custom applications.

10.3. Integration and device miniaturization

The seamless integration of piezoelectric composites into complete functional devices remains technologically and economically challenging [42]. Contact resistance at electrode interfaces, efficient electrical impedance matching between composite elements and power management circuits, and thermal management in densely integrated systems all present unresolved technical challenges. Future advancement requires development of integrated electrode materials, improved electrical contacting strategies, and sophisticated power conditioning electronics optimized specifically for low-frequency, variable-amplitude mechanical inputs characteristic of wearable and biomedical applications.

10.4. Materials sustainability and toxicity concerns

While significant progress has been made toward lead-free ceramic fillers, comprehensive life-cycle assessments of piezoelectric composite materials remain limited [2]. The synthesis, processing, recycling, and end-of-life environmental implications of complex ceramic-polymer systems

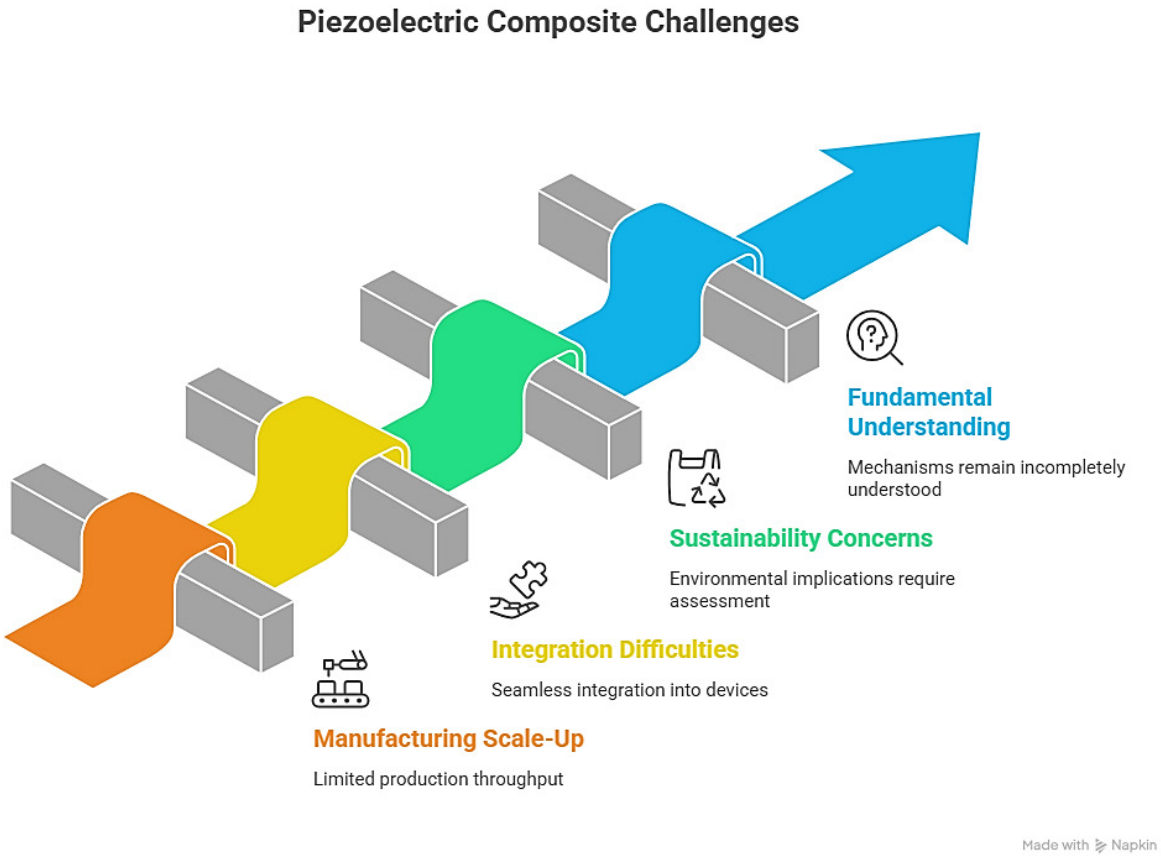

Fig. 23. The changing course of current and future challenges for the optimal use of piezoelectric composites.

require thorough investigation to ensure genuine sustainability advantages over conventional power sources. Development of bio-derived or biodegradable piezoelectric polymers represents an emerging frontier that could substantially reduce environmental footprint while expanding application domains into biomedical fields with strict biocompatibility requirements.

10.5. Fundamental understanding and multiscale modeling

Despite decades of research, the fundamental mechanisms governing piezoelectric response in nanostructured ceramic-polymer composites remain incompletely understood at the molecular and atomic scales [28]. Advanced computational methods including density functional theory, molecular dynamics simulations, and finite element modeling must be integrated with experimental characterization to develop predictive frameworks enabling rational materials design. Such multiscale modeling approaches would revolutionize the field by permitting computational optimization of complex composite architectures before experimental synthesis, substantially accelerating development timelines and reducing empirical screening requirements.

11. CONCLUSION

Piezoelectric polymer composites represent an advanced class of smart and multifunctional materials that uniquely combine the high piezoelectric response and dielectric properties of ceramic fillers with the flexibility, low density, and mechanical robustness of polymer matrices. This synergistic combination enables efficient electromechanical transduction while maintaining structural adaptability in the form of thin, lightweight, and large-area films.

A key advantage of these materials lies in their tunable architecture: by carefully selecting filler type, morphology, volume fraction, and spatial distribution within the polymer matrix, it is possible to precisely tailor dielectric, piezoelectric, thermal, and mechanical properties for specific applications. Such structural design flexibility allows optimization for sensors, actuators, and energy harvesting systems across diverse fields including consumer electronics, sport-instruments, automotive engineering, and biomedicine.

Emerging research trends focus on the development of multifunctional tricomposite systems incorporating multiple functional fillers, the adoption of environmentally friendly and lead-free materials, and the integration of advanced fabrication strategies—particularly additive manufacturing—to enable controlled microstructure de-

sign and improved device integration. Through intelligent structural engineering and materials selection, piezoelectric polymer composites continue to evolve toward higher performance, multifunctionality, and application-specific optimization.

REFERENCES

[1] C.R. Bowen, V.Yu. Topolov, H.A. Kim. The piezoelectric medium and its characteristics. In: *Modern Piezoelectric Energy-Harvesting Materials*. *Springer Series in Materials Science*. Vol. 238. Springer, Cham, 2016, pp. 1–22.

[2] S. Priya, H.-C. Song, Y. Zhou, R. Varghese, A. Chopra, S.-G. Kim, I. Kanno, L. Wu, D.S. Ha, J. Ryu, R.G. Polcawich. A review on piezoelectric energy harvesting: Materials, methods, and circuits. *Energy Harvesting and Systems*, 2017, vol. 4, no. 1, pp. 3–39.

[3] M.T. Sebastian, H. Jantunen. Polymer–ceramic composites of 0–3 connectivity for circuits in electronics: A review. *International Journal of Applied Ceramic Technology*, 2010, vol. 7, no. 4, pp. 415–434.

[4] V.V. Kochervinskii. Piezoelectricity in crystallizing ferroelectric polymers: Poly(vinylidene fluoride) and its copolymers (A review). *Crystallography Reports*, 2003, vol. 48, no. 4, pp. 649–675.

[5] G.V. Selicani, M. Mobin, V. Esposito, A.R. Insinga, A.B. Haugen. Shape engineering and manufacturing of piezoceramics for energy conversion—a review. *Journal of Physics: Energy*, 2025, vol. 7, no. 2, art. no. 022004.

[6] R.N. Joshua, A.R. Sakthivel. Reinforced polymer composite filaments in fused deposition modeling of 3D printing technology: A review. *Advanced Engineering Materials*, 2025, vol. 27, no. 9, art. no. 2402509.

[7] M. Habib, I. Lantgios, K. Hornbostel. A review of ceramic, polymer and composite piezoelectric materials. *Journal of Physics D: Applied Physics*, 2022, vol. 55, no. 42, art. no. 423002.

[8] O. Tokay, M. Yazıcı. A review of potassium sodium niobate and bismuth sodium titanate based lead free piezoceramics. *Materials Today Communications*, 2022, vol. 31, art. no. 103358.

[9] S. Sukumaran, S. Chatbouri, D. Rouxel, E. Tisserand, F. Thiebaud, T.B. Zineb. Recent advances in flexible PVDF based piezoelectric polymer devices for energy harvesting applications. *Journal of Intelligent Material Systems and Structures*, 2020, vol. 32, no. 7, pp. 746–780.

[10] X. Hu, S. Yu, B. Chu. Increased effective piezoelectric response of structurally modulated P(VDF-TrFE) film devices for effective energy harvesters. *Materials & Design*, 2020, vol. 192, art. no. 108700.

[11] K. Arlt, M. Wegener. Piezoelectric PZT / PVDF-copolymer 0-3 composites: aspects on film preparation and electrical poling. *IEEE Transactions on Dielectrics and Electrical Insulation*, 2010, vol. 17, no. 4, pp. 1178–1184.

[12] F. Levassort, A.C. Hladky-Hennion, H.L. Khanh, P. Tran-Huu-Hue, M. Lethiecq, M.P. Thi. 0-3 and 1-3 piezocomposites based on single crystal PMN-PT for transducer applications. *Advances in Applied Ceramics*, 2009, vol. 109, no. 3, pp. 162–168.

[13] C.R. Bowen, V.Yu. Topolov, Y. Zhang, A.A. Panich. 1-3-type composites based on ferroelectrics: Electromechanical coupling, figures of merit, and piezotechnical energy-harvesting applications. *Energy Technology*, 2018, vol. 6, no. 5, pp. 813–828.

[14] X. Song, L. He, W. Yang, Z. Wang, Z. Chen, J. Guo, H. Wang, L. Chen. Additive manufacturing of Bi-Continuous piezocomposites with triply periodic phase interfaces for combined flexibility and piezoelectricity. *Journal of Manufacturing Science and Engineering*, 2019, vol. 141, no. 11, art. no. 111004.

[15] S. Tian, Z. Zhao, B. Li, Y. Dai. Microstructural engineering for temperature-stable piezoresponse in KNN-based lead-free piezoceramics: a comprehensive review. *Microstructures*, 2026, vol. 6, art. no. 2026005.

[16] C.M. Costa, V.F. Cardoso, P. Martins, D.M. Correia, R. Gonçalves, P. Costa, V. Correia, C. Ribeiro, M.M. Fernandes, P.M. Martins, S. Lanceros-Méndez. Smart and multifunctional materials based on electroactive poly(vinylidene fluoride): Recent advances and opportunities in sensors, actuators, energy, environmental, and biomedical applications. *Chemical Reviews*, 2023, vol. 123, no. 19, pp. 11392–11487.

[17] X. Zhang, Y. Shen, Z. Shen, J. Jiang, L. Chen, C.-W. Nan. Achieving high energy density in PVDF-based polymer blends: Suppression of early polarization saturation and enhancement of breakdown strength. *ACS Applied Materials & Interfaces*, 2016, vol. 8, no. 40, pp. 27236–27242.

[18] H. Abdolmaleki, A.B. Haugen, K.B. Buhl, K. Daasbjerg, S. Agarwala. Interfacial engineering of PVDF-TrFE toward higher piezoelectric, ferroelectric, and dielectric performance for sensing and energy harvesting applications. *Advanced Science*, 2023, vol. 10, no. 6, art. no. 2205942.

[19] A. Habib, T. Fahmy, A. Almalki, M.M. Metwally. CERIA/PVDF/PVDF-HFP nanocomposite: Designing, characterization, optical, piezo- and pyroelectric properties for energy storage systems. *Journal of Inorganic and Organometallic Polymers and Materials*, 2025, vol. 35, no. 12, pp. 10080–10098.

[20] H. Kawai. The piezoelectricity of poly(vinylidene fluoride). *Japanese Journal of Applied Physics*, 1969, vol. 8, no. 7, art. no. 975.

[21] J. Su, Z.Y. Ma, J.I. Scheinbeim, B.A. Newman. Ferroelectric and piezoelectric properties of nylon 11/poly(vinylidene fluoride) bilaminate films. *Journal of Polymer Science Part B: Polymer Physics*, 1995, vol. 33, no. 1, pp. 85–91.

[22] S.C. Mathur, J.I. Scheinbeim, B.A. Newman. Piezoelectric properties and ferroelectric hysteresis effects in uniaxially stretched nylon-11 films. *Journal of Applied Physics*, 1984, vol. 56, no. 9, pp. 2419–2425.

[23] S. Anwar, M.H. Amiri, S. Jiang, M.M. Abolhasani, P.R.F. Rocha, K. Asadi. Piezoelectric nylon-11 fibers for electronic textiles, energy harvesting and sensing. *Advanced Functional Materials*, 2020, vol. 31, no. 4, art. no. 2004326.

[24] Z. Wang, Y. Duan, C. Liu, L. Wang, Z. Zhang, W. Zhao, X. Zhang, Y. Zhang, P. Fu, H. Cai, Z. Cui, X. Pang, Z.L. Dong, M. Liu. High-performance mechano-sensitive piezoelectric nanogenerator from post-treated nylon-11,11 textiles for energy harvesting and human motion monitoring. *ACS Applied Materials & Interfaces*, 2025, vol. 17, no. 5, pp. 8312–8326.

[25] S. Zhang, H. Zhang, J. Sun, N. Javanmardi, T. Li, F. Jin, Y. He, G. Zhu, Y. Wang, T. Wang, Z.-Q. Feng. A review of recent advances of piezoelectric poly-L-lactic acid for biomedical applications. *International Journal of Biological Macromolecules*, 2024, vol. 276, part 1, art. no. 133748.

[26] R. Schönlein, P. Bhattarai, M. Raef, X. Larrañaga, A. Poudel, M. Biggs, R. Aguirresarobe, J.M. Ugartemendia. Piezoelectric polylactic acid-based biomaterials: Fundamentals, challenges and opportunities in medical device design. *Biomaterials*, 2025, vol. 324, art. no. 123522.

[27] R. Schönlein, X. Larrañaga, M. Azkune, Y. Li, G. Liu, A.J. Müller, R. Aguirresarobe, J.M. Ugartemendia. The combined effects of optical purity, chain orientation, crystallinity, and dynamic mechanical activation as means to obtain highly piezoelectric polylactide materials. *ACS Applied Polymer Materials*, 2024, vol. 6, no. 13, pp. 7561–7571.

[28] X. Chen, X. Fu, Z. Chen, Z. Zhai, H. Miu, P. Tao. Multifunctional polyimide for packaging and thermal management of electronics: Design, synthesis, molecular structure, and composite engineering. *Nanomaterials*, 2025, vol. 15, no. 15, art. no. 1148.

[29] S. Yu, Y. Liu, C. Ding, X. Liu, Y. Liu, D. Wu, H. Luo, S. Chen. All-organic sandwich structured polymer dielectrics with polyimide and PVDF for high temperature capacitor application. *Journal of Energy Storage*, 2023, vol. 62, art. no. 106868.

[30] B. Gonzalo, J.L. Vilas, M. San Sebastián, T. Breczewski, M.A. Pérez-Jubindo, M.R. de la Fuente, M. Rodríguez, L.M. León. Electric modulus and polarization studies on piezoelectric polyimides. *Journal of Applied Polymer Science*, 2011, vol. 125, no. 1, pp. 67–76.

[31] Z. Dong, Q. He, D. Shen, Z. Gong, D. Zhang, W. Zhang, T. Ono, Y. Jiang. Microfabrication of functional polyimide films and microstructures for flexible MEMS applications. *Microsystems & Nanoengineering*, 2023, vol. 9, no. 1, art. no. 31.

[32] H. Wu, F. Zhuo, H. Qiao, L.K. Venkataraman, M. Zheng, S. Wang, H. Huang, B. Li, X. Mao, Q. Zhang. Polymer-/ceramic-based dielectric composites for energy storage and conversion. *Energy & Environment Materials*, 2021, vol. 5, no. 2, pp. 486–514.

[33] O.P. Prabhakar, R.K. Sahu. Tailoring molecular structure and electromechanical properties of polydimethylsiloxane elastomer for enhanced energy conversion efficiency. *Polymer Engineering and Science*, 2024, vol. 64, no. 10, pp. 4861–4876.

[34] M. Alexandre, C. Bessaguet, C. David, E. Dantras, C. Lacabanne. Piezoelectric properties of polymer/lead-free ceramic composites. *Phase Transitions*, 2016, vol. 89, no. 7–8, pp. 708–716.

[35] S.A. Muraina, M.A. Akinlabi, O. Fikayo, C.I. Collins, C.A. Chinonyerem. Design and properties of polymer–ceramic nanocomposites for dual energy storage and biomedical applications. *Asian Journal of Advanced Research and Reports*, 2025, vol. 19, no. 11, pp. 88–99.

[36] M. Acosta, N. Novak, V. Rojas, S. Patel, R. Vaish, J. Koruza, G.A. Rossetti Jr., J. Rödel. $BaTiO_3$-based piezoelectrics: Fundamentals, current status, and perspectives. *Applied Physics Reviews*, 2017, vol. 4, no. 4, art. no. 041305.

[37] T. Hoshina, S. Hatta, H. Takeda, T. Tsurumi. Grain size effect on piezoelectric properties of $BaTiO_3$ ceramics. *Japanese Journal of Applied Physics*, 2018, vol. 57, no. 9, art. no. 0902BB.

[38] Z.-Y. Shen, J.-F. Li. Enhancement of piezoelectric constant d_{33} in $BaTiO_3$ ceramics due to nano-domain structure. *Journal of the Ceramic Society of Japan*, 2010, vol. 118, no. 1382, pp. 940–943.

[39] H. Celebi, S. Duran, A. Dogan. The effect of core-shell $BaTiO_3$@SiO_2 on the mechanical and dielectric properties of PVDF composites. *Polymer-Plastics Technology and Materials*, 2022, vol. 61, no. 11, pp. 1191–1203.

[40] D. Maurya, S. Priya. Effect of bismuth doping on the dielectric and piezoelectric properties of $Ba_{1-x}Bi_xTiO_3$ lead-free ceramics. *Integrated Ferroelectrics*, 2015, vol. 166, no. 1, pp. 186–196.

[41] G. Dong, H. Fan, L. Liu, P. Ren, Z. Cheng, S. Zhang. Large electrostrain in $Bi_{1/2}Na_{1/2}TiO_3$-based relaxor ferroelectrics: A case study of $Bi_{1/2}Na_{1/2}TiO_3$-$Bi_{1/2}K_{1/2}TiO_3$-$Bi(Ni_{2/3}Nb_{1/3})O_3$ ceramics. *Journal of Materiomics*, 2020, vol. 7, no. 3, pp. 593–602.

[42] J. Lin, J. Qian, Y. Shi, S. Wang, J. Lin, G. Ge, Y. Hua, B. Shen, J. Zhai. Enhanced piezoelectric response attained by defect dipoles in $BiFeO_3$-based lead-free ceramics. *ACS Applied Materials & Interfaces*, 2024, vol. 16, no. 49, pp. 67959–67969.

[43] N. Bhadwal, R.B. Mrad, K. Behdinan. Review of zinc oxide piezoelectric nanogenerators: Piezoelectric properties, composite structures and power output. *Sensors*, 2023, vol. 23, no. 8, art. no. 3859.

[44] L. Legardinier, G. Ardila, I. Gélard, C. Jiménez, M. Weber, F. Donatinic, V. Consonni. Enhancement of the piezoelectric response of ZnO nanowires grown via PLI-MOCVD using post-deposition treatments through adjusted screening and surface effects. *Nanoscale*, 2025, vol. 17, no. 17, pp. 10835–10849.

[45] P.A. Upadhye, S.R. Chowdhury, V. Kumar, R. Ranjan, S. Kumar, S. Mondal, J. Oh, M. Misra. Hollow ZnO nanorod in PVDF matrix for high-performance sensing, vibration energy harvesting and wearable application. *Scientific Reports*, 2025, vol. 15, art. no. 19885.

[46] A.T. Le, M. Ahmadipour, S.-Y. Pung. A review on ZnO-based piezoelectric nanogenerators: Synthesis, characterization techniques, performance enhancement and applications. *Journal of Alloys and Compounds*, 2020, vol. 844, art. no. 156172.

[47] B.N. Kumar, T. Babu, B. Tiwari, R.N.P. Choudhary. Review on PZT as a mechanical engineering material. *Ferroelectrics*, 2024, vol. 618, no. 1, pp. 125–138.

[48] Y. Shi, R. He, B. Zhang, Z. Zhong. Revisiting the phase diagram and piezoelectricity of lead zirconate titanate from first principles. *Physical Review B*, 2024, vol. 109, no. 17, art. no. 174104.

[49] Y. Huang, L. Zhang, R. Jing, M. Tang, D. Alikin, V. Shur, X. Wei, L. Jin. Lead zirconate titanate-based ceramics with high piezoelectricity and broad usage temperature range. *Chemical Engineering Journal*, 2023, vol. 477, art. no. 147192.

[50] D. Wang, Z. Fan, G. Rao, G. Wang, Y. Liu, C. Yuan, T. Ma, D. Li, X. Tan, Z. Lu, A. Feteira, S. Liu, C. Zhou, S. Zhang. Ultrahigh piezoelectricity in lead-free piezoceramics by synergistic design. *Nano Energy*, 2020, vol. 76, art. no. 104944.

[51] J. Li, W. Ma, S. Wang, J. Guo, J. Hong, S. Yang. Improving the performance of flexible composites based on 3-3 interconnected skeletons for piezoelectric energy harvesting. *Ceramics International*, 2023, vol. 49, no. 14, pp. 23349–23357.

[52] X. Lin, X. Zhang, X. Fei, C. Wang, H. Liu, S. Huang. Flexible three-dimensional interconnected PZT skeleton based piezoelectric nanogenerator for energy harvesting. *Ceramics International*, 2023, vol. 49, no. 16, pp. 27526–27534.

[53] A. Adaval, F. Akram, R. Janardhana, Z. Guler, N. Jackson. Development of PVDF/AlN nanocomposites with

enhanced thermal properties for piezoelectric applications. Smart Materials and Structures, 2025, vol. 34, no. 6, art. no. 065016.
[54] W. Peng, J. Chang, J. Zhao, D. Wang, Z. Liu, G. Wang, S. Dong. Enhanced piezoelectric properties and thermal stability of $LiNbO_3$-modified PNN–PZT ceramics. *Journal of Materiomics*, 2023, vol. 10, no. 5, pp. 995–1003.
[55] T. Prabhakaran, J. Hemalatha. Poly(vinylidene fluoride)-based magnetoelectric polymer nanocomposite films. In: S. Lanceros-Méndez, P. Martins (Eds.). *Magnetoelectric Polymer-Based Composites: Fundamentals and Applications*. Wiley, 2017, pp. 87–113.
[56] K. Kim, J.L. Middlebrook, J.E. Chen, W. Zhu, S. Chen, D.J. Sirbuly. Tunable surface and matrix chemistries in optically printed (0–3) piezoelectric nanocomposites. *ACS Applied Materials & Interfaces*, 2016, vol. 8, no. 49, pp. 33394–33398.
[57] R. Mitkus, M. Sinapius. Piezoelectric ceramic/photopolymer composites curable with UV light: Viscosity, curing depth, and dielectric properties. *Journal of Composites Science*, 2022, vol. 6, no. 7, art. no. 212.
[58] N. Kashaninejad, N.-T. Nguyen, W.K. Chan. Engineering micropatterned surfaces for controlling the evaporation process of sessile droplets. *Technologies*, 2020, vol. 8, no. 2, art. no. 29.
[59] A. Magnani, S. Capaccioli, B. Azimi, S. Danti, M. Labardi. Local piezoelectric response of polymer/ceramic nanocomposite fibers. *Polymers*, 2022, vol. 14, no. 24, art. no. 5379.
[60] D. Liu, W. Yao, C. Zhou, J. Zhang. Electromechanical properties and temperature stability of 1-3 type PZT/epoxy piezoelectric composite. *IOP Conference Series: Materials Science and Engineering*, 2019, vol. 678, no. 1, art. no. 012136.
[61] G.-S. Chen, H.-C. Liu, Y.-C. Lin, Y.-L. Lin. Experimental analysis of 1-3 piezocomposites for high-intensity focused ultrasound transducer applications. *IEEE Transactions on Biomedical Engineering*, 2012, vol. 60, no. 1, pp. 128–134.
[62] R. Sahore, B.L. Armstrong, X. Tang, C. Liu, K. Owensby, S. Kalnaus, X.C. Chen. Role of scaffold architecture and excess surface polymer layers in a 3D-interconnected ceramic/polymer composite electrolyte. *Advanced Energy Materials*, 2023, vol. 13, no. 19, art. no. 2203663.
[63] A. Safari. Overcoming the limits of piezoelectric composites. *National Science Review*, 2023, vol. 10, no. 9, art. no. nwad205.
[64] Z. Wu, Y. Peng, Q. Guo, H. Zhou, L. Gong, Z. Liu, Q. Zhang, Y. Chen. Multilayer heterogeneous dielectric films with simultaneously improved dielectric constant and breakdown strength. *Materials Today Communications*, 2022, vol. 32, art. no. 103857.
[65] U. Yaqoob, G.-S. Chung. Effect of reduced graphene oxide on the energy harvesting performance of P(VDF-TrFE)-$BaTiO_3$ nanocomposite devices. *Smart Materials and Structures*, 2017, vol. 26, no. 9, art. no. 095060.
[66] M. Yan, S. Liu, Q. Xu, Z. Xiao, X. Yuan, K. Zhou, D. Zhang, Q. Wang, C. Bowen, J. Zhong, Y. Zhang. Enhanced energy harvesting performance in lead-free multi-layer piezoelectric composites with a highly aligned pore structure. *Nano Energy*, 2022, vol. 106, art. no. 108096.
[67] J.I. Roscow, H. Pearce, H. Khanbareh, S. Kar-Narayan, C.R. Bowen. Modified energy harvesting figures of merit for stress- and strain-driven piezoelectric systems. *The European Physical Journal Special Topics*, 2019, vol. 228, no. 7, pp. 1537–1554.
[68] M.M. Abolhasani, M. Naebe, M.H. Amiri, K. Shirvanimoghaddam, S. Anwar, J.J. Michels, K. Asadi. Hierarchically structured porous piezoelectric polymer nanofibers for energy harvesting. *Advanced Science*, 2020, vol. 7, no. 13, art. no. 2000517.
[69] J. Li, Y. Yang, H. Jiang, Y. Wang, Y. Chen, S. Jiang, J.-M. Wu, G. Zhang. 3D interpenetrating piezoceramic-polymer composites with high damping and piezoelectricity for impact energy-absorbing and perception. *Composites Part B: Engineering*, 2022, vol. 232, art. no. 109617.
[70] Z. He, F. Rault, M. Lewandowski, E. Mohsenzadeh, F. Salaün. Electrospun PVDF nanofibers for piezoelectric applications: A review of the influence of electrospinning parameters on the β phase and crystallinity enhancement. *Polymers*, 2021, vol. 13, no. 2, art. no. 174.
[71] A.D. Hussein, R.S. Sabry, O.A.A. Dakhil, R. Bagherzadeh. Effect of adding BaTiO3 to PVDF as nano generator. *Journal of Physics: Conference Series*, 2019, vol. 1294, no. 2, art. no. 022012.
[72] X. Wei, K. Xu, Y. Wang, Z. Zhang, Z. Chen. 3D printing of flexible $BaTiO_3$/polydimethylsiloxane piezocomposite with aligned particles for enhanced energy harvesting. *ACS Applied Materials & Interfaces*, 2024, vol. 16, no. 9, pp. 11740–11748.
[73] S. Saadon, O. Sidek. Environmental vibration-based MEMS piezoelectric energy harvester (EVMPEH). In: *2011 Developments in E-systems Engineering*. Dubai, United Arab Emirates, 2011, pp. 511–514.
[74] H.J. Chilabi, H. Salleh, E.E. Supeni, A. As'arry, K.A.M. Rezali, A.B. Atrah. Harvesting energy from planetary gear using piezoelectric material. *Energies*, 2020, vol. 13, no. 1, art. no. 223.
[75] S.K. Sood. *Piezoelectric micro power generator (PMPG): a MEMS based energy scavenger*. Thesis (M. Eng.). Massachusetts Institute of Technology, Dept. of Electrical Engineering and Computer Science, 2003.
[76] W. Zhou, D. Du, Q. Cui, C. Lu, Y. Wang, Q. He. Recent research progress in piezoelectric vibration energy harvesting technology. *Energies*, 2022, vol. 15, no. 3, art. no. 947.
[77] Q.L. Zhao, Z.X. Li, G.P. He, M.S. Cao, D.W. Cao, J.J. Di. Fabrication and characterization of a high Q-factor microcantilever enhanced by lead zirconate titanate thick film. *Journal of the Chinese Ceramic Society*, 2014, vol. 42, pp. 65–69.
[78] Z.L. Wang, J. Song. Piezoelectric nanogenerators based on zinc oxide nanowire arrays. *Science*, 2006, vol. 312, no. 5771, pp. 242–246.
[79] B. ElZein, Y. Yao, A.S. Barham, E. Dogheche, G.E. Jabbour. Toward the growth of self-catalyzed ZnO nanowires perpendicular to the surface of silicon and glass substrates, by pulsed laser deposition. *Materials*, 2020, vol. 13, no. 19, art. no. 4427.
[80] R. Latif, M.M. Noor, J. Yunas, A.A. Hamzah. Mechanical energy sensing and harvesting in micromachined polymer-based piezoelectric transducers for fully implanted hearing systems: A review. *Polymers*, 2021, vol. 13, no. 14, art. no. 2276.
[81] X. Wang, J. Song, J. Liu, Z.L. Wang. Direct-current nanogenerator driven by ultrasonic waves. *Science*, 2007, vol. 316, no. 5821, pp. 102–105.
[82] Y.M. Wang, Q. Zeng, L. He, P. Yin, Y. Sun, W. Hu, R. Yang. Fabrication and application of biocompatible nanogenerators. *iScience*, 2021, vol. 24, no. 4, art. no. 102274.

[83] S. Siddiqui, D.-I. Kim, L.T. Duy, M.T. Nguyen, S. Muhammad, W.-S. Yoon, N.-E. Lee. High-performance flexible lead-free nanocomposite piezoelectric nanogenerator for biomechanical energy harvesting and storage. *Nano Energy*, 2015, vol. 15, pp. 177–185.

[84] W. Wu, L. Cheng, S. Bai, W. Dou, Q. Xu, Z. Wei, Y. Qin. Electrospinning lead-free $0.5Ba(Zr_{0.2}Ti_{0.8})O_3$–$0.5(Ba_{0.7}Ca_{0.3})TiO_3$ nanowires and their application in energy harvesting. *Journal of Materials Chemistry A*, 2013, vol. 1, no. 25, pp. 7332–7338.

[85] Z. Zhou, C.C. Bowland, M.H. Malakooti, H. Tang, H.A. Sodano. Lead-free $0.5Ba(Zr_{0.2}Ti_{0.8})O_3$–$0.5(Ba_{0.7}Ca_{0.3})TiO_3$ nanowires for energy harvesting. *Nanoscale*, 2016, vol. 8, no. 9, pp. 5098–5105.

[86] C. Baek, J.H. Yun, J.E. Wang, C.K. Jeong, K.J. Lee, K.-I. Park, D.K. Kim. A flexible energy harvester based on a lead-free and piezoelectric BCTZ nanoparticle–polymer composite. *Nanoscale*, 2016, vol. 8, no. 40, pp. 17632–17638.

[87] R. Zhu, J. Jiang, Z. Wang, Z. Cheng, H. Kimura. High output power density nanogenerator based on lead-free $0.96(K_{0.48}Na_{0.52})(Nb_{0.95}Sb_{0.05})O_3$–$0.04Bi_{0.5}(Na_{0.82}K_{0.18})_{0.5}ZrO_3$ piezoelectric nanofibers. *RSC Advances*, 2016, vol. 6, no. 71, pp. 66451–66456.

[88] J. Yan, Y.G. Jeong. High performance flexible piezoelectric nanogenerators based on $BaTiO_3$ nanofibers in different alignment modes. *ACS Applied Materials & Interfaces*, 2016, vol. 8, no. 24, pp. 15700–15709.

[89] D. Shen, J.-H. Park, J.H. Noh, S.-Y. Choe, S.-H. Kim, H.C. Wikle III, D.-J. Kim. Micromachined PZT cantilever based on SOI structure for low frequency vibration energy harvesting. *Sensors and Actuators A: Physical*, 2009, vol. 154, no. 1, pp. 103–108.

[90] W. Wu, S. Bai, M. Yuan, Y. Qin, Z.L. Wang, T. Jing. Lead zirconate titanate nanowire textile nanogenerator for wearable energy-harvesting and self-powered devices. *ACS Nano*, 2012, vol. 6, no. 7, pp. 6231–6235.

[91] R.E. Newnham, D.P. Skinner, L.E. Cross. Connectivity and piezoelectric-pyroelectric composites. *Materials Research Bulletin*, 1978, vol. 13, no. 5, pp. 525–536.

[92] R. Sun, L. Wang, Y. Zhang, C. Zhong. Characterization of 1-3 piezoelectric composite with a 3-tier polymer structure. *Materials*, 2020, vol. 13, no. 2, art. no. 397.

[93] W.A. Smith. The role of piezocomposites in ultrasonic transducers. In: *Proceedings of IEEE Ultrasonics Symposium*. Montreal, QC, Canada, 1989, pp. 755–766.

[94] A. Safari, E.K. Akdogan. *Piezoelectric and Acoustic Materials for Transducer Applications*. Springer, 2008.

[95] L. Persano, S.K. Ghosh, D. Pisignano. Enhancement and function of the piezoelectric effect in polymer nanofibers. *Accounts of Materials Research*, 2022, vol. 3, no. 9, pp. 900–912.

[96] M. Jalali, E. Elnabawy, A.A. Sallam, S. Jaradat, A. Al-Dubai, N. Shehata, I. Shyha. Advancements in polymeric piezoelectric nanofiber for energy harvesting applications: A scoping review. *Fibers and Polymers*, 2025, vol. 27, pp. 1–23.

[97] M.A. Bonakdar, D. Rodrigue. Electrospinning: Processes, structures, and materials. *Macromol*, 2024, vol. 4, no. 1, pp. 58–103.

[98] R.K. Singh, S.W. Lye, J. Miao. Holistic investigation of the electrospinning parameters for high percentage of β-phase in PVDF nanofibers. *Polymer*, 2020, vol. 214, art. no. 123366.

[99] A.I. Emara, A.F. Shahba, K. Nassar, T. Hamouda. Optimizing solution blow spinning of PVDF nanofibers: A study on morphology, crystalline phases, and piezoelectric performance. *Egyptian Journal of Chemistry*, 2024, vol. 67, no. 13, pp. 1–10.

[100] W.T. Nugroho, Y. Dong, A. Pramanik. 3D printing composite materials: A comprehensive review. In: I.-M. Low, Y. Dong (Eds.). *Composite Materials*. Elsevier, 2021, pp. 65–115.

[101] H. Kim, F. Torres, D. Villagran, C. Stewart, Y. Lin, T.B. Tseng. 3D printing of $BaTiO_3$/PVDF composites with electric in situ poling for pressure sensor applications. *Macromolecular Materials and Engineering*, 2017, vol. 302, no. 11, art. no. 1700229.

[102] H. Wang, Q. Lai, D. Zhang, X. Li, J. Hu, H. Yuan. A systematic study on digital light processing 3D printing of 0-3 ceramic composites for piezoelectric metastructures. *Research*, 2025, vol. 8, art. no. 0595.

[103] L. Pang, N.C. Paxton, J. Ren, F. Liu, H. Zhan, M.A. Woodruff, A. Bo, Y. Gu. Development of mechanically enhanced polycaprolactone composites by a functionalized titanate nanofiller for melt electrowriting in 3D printing. *ACS Applied Materials & Interfaces*, 2020, vol. 12, no. 42, pp. 47993–48006.

[104] J. Liu, Y. Gao, D. Cao, L. Zhang, Z. Guo. Nanoparticle dispersion and aggregation in polymer nanocomposites: Insights from molecular dynamics simulation. *Langmuir*, 2011, vol. 27, no. 12, pp. 7926–7933.

[105] R.D. Kroshefsky, J.L. Price, D. Mangaraj. Role of compatibilization in polymer nanocomposites. *Rubber Chemistry and Technology*, 2009, vol. 82, no. 3, pp. 340–368.

[106] H.T.T. Nong, A.N. Nguyen, J. Solard, A. Gomez, S. Mercone. Robust piezoelectric coefficient recovery by nano-inclusions dispersion in un-poled PVDF–$Ni_{0.5}Zn_{0.5}Fe_2O_4$ ultra-thin films. *Applied Sciences*, 2022, vol. 12, no. 3, art. no. 1589.

[107] A. Zarinwall, R. Mitkus, A. Marth, V. Maurer, M. Sinapius, G. Garnweitner. Processing of 3-(trimethoxysilyl) propyl methacrylate (TMSPM) functionalized barium titanate/photopolymer composites: Functionalization and process parameter investigation. *Journal of Composites Science*, 2023, vol. 7, no. 2, art. no. 47.

[108] V. Bouad, M. Girardot, V. Ladmiral, S. Barrau. Piezoelectric fluorinated polymer composites: A review on coupling agents at the filler/matrix interface. *Polymer Composites*, 2024, vol. 45, no. 5, pp. 3861–3882.

[109] L. Song, S. Glinsek, E. Defay. Toward low-temperature processing of lead zirconate titanate thin films: Advances, strategies, and applications. *Applied Physics Reviews*, 2021, vol. 8, no. 4, art. no. 041312.

[110] J. Guo, S.S. Berbano, H. Guo, A.L. Baker, M.T. Lanagan, C.A. Randall. Cold sintering process of composites: Bridging the processing temperature gap of ceramic and polymer materials. *Advanced Functional Materials*, 2016, vol. 26, no. 39, pp. 7115–7121.

[111] S. Salmanov, D. Kuščer, M. Otoničar. Cold sintering of perovskite–perovskite particulate composite based on $K_{0.5}Na_{0.5}NbO_3$ and $BiFeO_3$. *Informacije MIDEM*, 2024, vol. 51, no. 3, pp. 167–176.

[112] D. Kopeliovich. Advances in the manufacture of ceramic matrix composites using infiltration techniques. In: I.M. Low (Ed.). *Advances in Ceramic Matrix Composites*. Woodhead Publishing, 2014, pp. 79–108.

[113] S. Gupta, D. Wang, S. Shetty, A. Meddeb, S. Dursun, C.A. Randall, S. Trolier-McKinstry. Cold sintering of

PZT 2-2 composites for high frequency ultrasound transducer arrays. *Actuators*, 2021, vol. 10, no. 9, art. no. 235.
[114] D.I. Makarev, A.N. Reznichenko, A.N. Rybyanets, A.N. Shvetsova, L.A. Reznichenko. Structural features and electrophysical properties of the "piezoceramic-polymer" composites. *Ferroelectrics*, 2022, vol. 591, no. 1, pp. 60–64.
[115] A. Kumar, A. Tezcan, Z. Li, R. Yang, F. Bouville, G. Poulin-Vittrant, H. Khanbareh, J. Roscow, S. Deville, C. Bowen. Freeze-cast porous textured $BaTiO_3$–polymer composites for energy harvesting applications. *ACS Applied Energy Materials*, 2025, vol. 8, no. 15, pp. 11437–11446.
[116] V. Pal, A.K. Singh, P.K. Swain. New developments in piezoelectric polymeric composite materials for environmental energy usages. In: P. Das, S. Das (Eds.). *Novel polymeric materials for environmental applications*. World Scientific Publishing, 2023, pp. 411–456.
[117] F. Mokhtari, B. Azimi, M. Salehi, S. Hashemikia, S. Danti. Recent advances of polymer-based piezoelectric composites for biomedical applications. *Journal of the Mechanical Behavior of Biomedical Materials*, 2021, vol. 122, art. no. 104669.
[118] X. Lin, F. Yu, X. Zhang, W. Li, Y. Zhao, X. Fei, Q. Li, C. Yang, S.-F. Huang. Wearable piezoelectric films based on MWCNT-$BaTiO_3$/PVDF composites for energy harvesting, sensing, and localization. *ACS Applied Nano Materials*, 2023, vol. 6, no. 13, pp. 11955–11965.
[119] A. Bagla, K. Hembram, F. Rault, F. Salaün, S. Sundarrajan, S. Ramakrishna, S. Mitra. ZnO@C/PVDF electrospun membrane as a piezoelectric nanogenerator for wearable applications. *The Journal of Physical Chemistry C*, 2025, vol. 129, no. 12, pp. 5808–5820.
[120] X. Zhou, X. Chen, B. Yang, S. Luo, M. Guo, N. An, H. Tian, X. Li, J. Shao. Advancements in functionalizable metal-organic frameworks for flexible sensing electronics. *Advanced Functional Materials*, 2025, vol. 35, no. 32, art. no. 2501683.
[121] S.A. Graham, A. Kurakula, V.S. Kavarthapu, J.K. Lee, P. Manchi, M.V. Paranjape, J.S. Yu. Metal-organic framework embedded electrospun fibrous membranes-based hybrid nanogenerators with hierarchical modified polyamide films for mechanical energy harvesting and IoT applications. *Advanced Functional Materials*, 2025, vol. 36, no. 10, art. no. 2507128.
[122] C. Hu, K. Behdinan, R. Moradi-Dastjerdi. PVDF energy harvester for prolonging the battery life of cardiac pacemakers. *Actuators*, 2022, vol. 11, no. 7, art. no. 187.
[123] M. Khazaee, S. Riahi, A. Rezania. Conceptual piezoelectric-based energy harvester from in vivo heartbeats' cyclic kinetic motion for leadless intracardiac pacemakers. *Micromachines*, 2024, vol. 15, no. 9, art. no. 1133.
[124] G. Hwang, H. Park, J.-H. Lee, S. Oh, K.-I. Park, M. Byun, H. Park, G. Ahn, C.K. Jeong, K. No, H. Kwon, S.-G. Lee, B. Joung, K.J. Lee. Self-powered cardiac pacemaker enabled by flexible single crystalline PMN-PT piezoelectric energy harvester. *Advanced Materials*, 2014, vol. 26, no. 28, pp. 4880–4887.
[125] F. Mokhtari, G.M. Spinks, C. Fay, Z. Cheng, R. Raad, J. Xi, J. Foroughi. Wearable electronic textiles from nanostructured piezoelectric fibers. *Advanced Materials Technologies*, 2020, vol. 5, no. 4, art. no. 1900900.
[126] H. Chen, M. Chen, L. Sun, G. Wang, J. Zhong, W. Guan. Piezoelectric-triboelectric coupling enhanced hybrid nanogenerator for flexible motion sensing. *ACS Applied Nano Materials*, 2025, vol. 8, no. 24, pp. 12693–12705.
[127] F. Mokhtari, Z. Cheng, R. Raad, J. Xi, J. Foroughi. Piezofibers to smart textiles: A review on recent advances and future outlook for wearable technology. *Journal of Materials Chemistry A*, 2020, vol. 8, no. 19, pp. 9496–9522.
[128] P. Costa, J. Nunes-Pereira, N. Pereira, N. Castro, S. Gonçalves, S. Lanceros-Mendez. Recent progress on piezoelectric, pyroelectric, and magnetoelectric polymer-based energy-harvesting devices. *Energy Technology*, 2019, vol. 7, no. 7, art. no. 1800852.
[129] X. Chen, S. Xu, N. Yao, Y. Shi. 1.6 V nanogenerator for mechanical energy harvesting using PZT nanofibers. *Nano Letters*, 2010, vol. 10, no. 6, pp. 2133–2137.
[130] J. Nunes-Pereira, V. Sencadas, V. Correia, V.F. Cardoso, W. Han, J.G. Rocha, S. Lanceros-Méndez. Energy harvesting performance of $BaTiO_3$/poly(vinylidene fluoride–trifluoroethylene) spin coated nanocomposites. *Composites Part B: Engineering*, 2014, vol. 72, pp. 130–136.
[131] C. Chang, V.H. Tran, J. Wang, Y.-K. Fuh, L. Lin. Direct-write piezoelectric polymeric nanogenerator with high energy conversion efficiency. *Nano Letters*, 2010, vol. 10, no. 2, pp. 726–731.
[132] C. Pan, L. Dong, G. Zhu, S. Niu, R. Yu, Q. Yang, Y. Liu, Z.L. Wang. High-resolution electroluminescent imaging of pressure distribution using a piezoelectric nanowire LED array. *Nature Photonics*, 2013, vol. 7, no. 9, pp. 752–758.
[133] R. Ding, H. Liu, X. Zhang, J. Xiao, R. Kishor, H. Sun, B. Zhu, G. Chen, F. Gao, X. Feng, J. Chen, X. Chen, X. Sun, Y. Zheng. Flexible piezoelectric nanocomposite generators based on formamidinium lead halide perovskite nanoparticles. *Advanced Functional Materials*, 2016, vol. 26, no. 42, pp. 7708–7716.
[134] M. Tabassum, Q. Zia, J. Li, M.T. Khawar, S. Aslam, L. Su. $FAPbBr_3$ perovskite nanocrystals embedded in poly(L-lactic acid) nanofibrous membranes for enhanced air and water stability. *Membranes*, 2023, vol. 13, no. 3, art. no. 279.
[135] J.J.H. Paulides, J.W. Jansen, L. Encica, E.A. Lomonova, M. Smit. Power from the people. *IEEE Industry Applications Magazine*, 2011, vol. 17, no. 5, pp. 20–26.
[136] J. Zhang, J. Wang, C. Zhong, Y. Zhang, Y. Qiu, L. Qin. Flexible electronics: Advancements and applications of flexible piezoelectric composites in modern sensing technologies. *Micromachines*, 2024, vol. 15, no. 8, art. no. 982.

УДК 53.081.7

Стратегии архитектурного проектирования керамико–полимерных гибридных пьезоэлектрических композитов для повышения эффективности энергосбора

А. Джабери, Е.Н. Дресвянина

Институт текстиля и моды, Санкт-Петербургский государственный университет промышленных технологий и дизайна, ул. Большая Морская, д. 18, Санкт-Петербург, 191186, Россия

Аннотация. Керамико-полимерные пьезоэлектрические композиты объединяют высокую пьезоэлектрическую активность сегнетоэлектрических керамик с механической гибкостью и долговечностью полимеров, формируя ключевую материаловедческую платформу для систем энергосбора следующего поколения. В настоящем обзоре критически анализируются последние достижения в области гибридных композитов для преобразования механической энергии в электрическую с акцентом на стратегии архитектурного проектирования, определяющие взаимосвязи «структура–свойства–эксплуатационные характеристики». Особое внимание уделяется типам связности фаз (0–3, 1–3 и 3–3) и современным подходам к инженерии структуры, включая ориентированные керамические сети, пористые каркасы, структуры «ядро–оболочка», градиентные конфигурации и функционализацию межфазных границ, которые повышают эффективность передачи механических напряжений, электромеханическое сопряжение и плотность мощности при одновременном снижении хрупкости и диэлектрических потерь. Оцениваются системы на основе свинецсодержащих (например, PZT) и бессвинцовых (например, BTO, KNN) керамик в сочетании с гибкими полимерными матрицами, такими как PVDF и его сополимеры, для применения в условиях низкочастотных вибраций, носимой электронике, мониторинге состояния конструкций и автономных сенсорных системах. Рассматриваются масштабируемые методы изготовления (литьё с направленным замораживанием, электроспиннинг и 3D-печать), а также методы многополевого моделирования, наряду с основными проблемами: стабильностью поляризации, усталостной прочностью, межфазным расслоением и долговременной надёжностью. Обзор формирует единый подход к архитектурной оптимизации и определяет стратегические направления создания высокоэффективных, прочных и экологически устойчивых систем энергосбора.

Ключевые слова: керамико–полимерные пьезоэлектрические композиты; сбор энергии; архитектура композитов; связность (0–3, 1–3, 3–3); мониторинг состояния конструкций